Erasmus Mundus Master in Membrane Engineering for a Sustainable World EM3E-4SW

Synthesis and Characterization of Micro-Patterned Thin Film Composite (TFC) Membranes for Water Treatment

Dissertation for obtaining the master's degree in Membrane Engineering

Erasmus Mundus Master in Membrane Engineering for a Sustainable World

(2018-20)

Dharmjeet MADHAV

14-07-2020

KU Leuven, Belgium

Universidad Zaragoza, Spain

Supervisor (s):

Prof. Dr. Ivo Vankelecom

KU Leuven, Belgium

Overseer (s):

Prof. Dr. Reyes Mallada

Universidad Zaragoza, Spain

With the support of the Erasmus+ Programme of the European Union

www.em3e-4sw.eu

The Erasmus Mundus Master in Membrane Engineering for a Sustainable Word (EM3E-4SW) is an education programme financed by the European Commission - Education, Audiovisual and Culture Executive Agency (EACEA), under Project Number-574441-EPP-1-2016-1-FR-EPPKA1-JMD-MOB. It is also supported by the European Membrane Society (EMS), the European Membrane House (EMH), and a large international network of industrial companies, research centers, and universities.

The EM3E-4SW education programme has been funded with support from the European Commission. This publication reflects the views only of the author, and the Commission cannot be held responsible for any use which may be made of the information contained therein.

El programa educativo EM3E-4SW ha sido financiado con el apoyo de la Comisión Europea. Esta publicación refleja solo las opiniones del autor, y la Comisión no se hace responsable del uso que pueda hacerse de la información contenida en el mismo.

Le programme d'éducation EM3E-4SW a été financé avec le soutien de la Commission européenne. Cette publication n'engage que son auteur et la Commission ne peut être tenue responsable de l'usage qui pourrait être fait des informations qui y sont contenues.

The master involves 6 High Education Institutions of 5 European countries: Université de Montpellier (France, coordinating organisation), Université Toulouse 3 Paul Sabatier (Toulouse, France), University of Chemistry and Technology Prague (Czech Republic), Universidad de Zaragoza (Spain), University of Twente (Netherlands) and Universidade Nova de Lisboa (Portugal). Associated partners are the Università della Calabria (Italy) and the Katholieke Universiteit Leuven (Belgium).

Acknowledgements

This thesis was adventurous, mysterious for its endless fluctuations. Fluctuations that forged the resilient young researcher that I am today. Of course, none of this could have happened if it was not for the people I encountered throughout this process and supported me generously.

I would begin by thanking Professor Ivo Vankelecom for his trust and providing me this opportunity of thesis in his research group. It was an honour to be among his solid research team. A particular mention goes to Ms. Ayesha who's been my daily supervisor. A PhD student I look up to; she has been incredibly supportive, humble, and generous in rapidly responding to all my queries throughout the realization of this project. Prof. Ivo, Ms. Ayesha, thank you very much. I would also like to thank the administrative staff and other researchers of the membrane technology group for their unconditional support.

My stay at KU Leuven has been a delight with the former research group members who've generously guided me and paved the way to the decisions I settled for, in my career. Abaynesh, Lisendra, Maxime, Maarten, Matthias, Emad and others, thank you for all your guidance and supports.

My gratitude is extended to all professors and administration people of EM3E-4SW master's program who've prepared me with solid theoretical foundation in membranes and helped me with the necessary technical issues. They all have been inspiring, encouraging and helpful.

I would like to thank my colleagues of EM3E-4SW with whom I shared fun and adventurous memories specially Irfan, Fatima, Mizan, Rafiul and all others. A special mention goes to Sara Chergaoui for the endless scientific discussions if not arguments we had particularly during thesis times. Her positive energy made the Corona wave less intense, that I could have withstood on my own. Thank you. Special thanks to my friends and colleagues from IIT Roorkee back in India for their constant support. Thank you, my friend Florian, for giving me a nice company during this stay in Leuven. Alok my friend, I can't thank you much for always being there for me whenever I needed any help.

Finally, to my family, my mother, father, sister and brother. Thank you for your unconditional love and support. Your encouragement was key to overcome all difficulties. I cannot thank you enough.

Dharmjeet Madhav, July 2020

Abstract

Thin film composite (TFC) membranes, mostly used in reverse osmosis and nanofiltration are critical for water treatment and provide clean and desalinated water to millions on daily basis. The two main limitations: fouling and low permeance of these membranes greatly affect their performance and sustainability. Several measures have been taken for membrane fouling mitigation including chemical, physical and hydrodynamic methods. Recently, patterned membranes have been evolved as an innovative tool for fouling mitigation. However, the synthesis procedure for patterned membranes has not been developed at a scale-up level. Lately, Prof. Vankelecom's research group (KU Leuven) has introduced a non-solvent spray assisted phase inversion (s-NIPS) as an efficient synthesis procedure for patterned membranes. s-NIPS makes the use of a patterned casting knife combined with modified non-solvent spray assisted phase inversion process. It overcomes the limitations of previously used methods such as phase separation micromolding (PSμM) and imprinting lithography (IL) as phase separation induces from the pattern side and no reduction in pore size is observed. Previous studies for patterned TFC membranes have only managed to create a top selective layer above patterned UF supports with heights in the range of 160 nm to 5 μm which limits the potential advantages of such membranes. s-NIPS patterned supports can significantly enhance the intrinsic low permeance of such NF/RO membranes by producing UF supports with higher pattern heights up to 180 μm. Hence, in this study, a defect-free thin film polyamide layer was developed over s-NIPS micro-patterned supports through interfacial polymerization (IP). In order to achieve this, several parameters were explored including effect of monomer concentrations, effect of pattern height, removal of excess monomer solution from the valleys before IP, effect of UF polymer support and spin assisted layer by layer thin film deposition. It was found that the 1, 2 and 3 layered TFC membrane could give a maximum of ca. 85, 96 and 97 % $MgSO_4$ retention respectively at enhanced permeance. Furthermore, 2 layered spin assisted IP with 2 wt% MPD and 0.1 wt% TMC concentration was found to be optimum for PSf_{500} supports (polysulfone supports prepared using casting knife with pattern height 500 μm) with 94% $MgSO_4$ retention at the permeance of 1.66 LMH/bar.

Keywords: Thin film composite membranes, TFC membranes, Patterned membranes, Water treatment, Fouling mitigation

Resumen

Las membranas de compuesto de película delgada (TFC), utilizadas principalmente en ósmosis inversa y nanofiltración, son críticas para el tratamiento de aguas y proporcionan agua limpia y desalinizada a millones de personas diariamente. Las dos limitaciones principales: la colmatación y la baja permeabilidad de estas membranas afectan en gran medida su rendimiento y sostenibilidad. Diferentes métodos químicos, físicos e hidrodinámicos han sido utilizados para mitigar la colmatación de la membrana. Recientemente, las membranas estampadas se han desarrollado como una herramienta innovadora para la mitigación de la colmatación. Sin embargo, el procedimiento de fabricación a gran escala de membranas estampadas no ha sido desarrollado. Últimamente, el grupo de investigación del profesor Vankelecom (KU Leuven) ha dado a conocer una inversión de fase asistida por atomización sin solvente (s-NIPS) como un procedimiento de síntesis eficiente para membranas estampadas. s-NIPS utiliza una cuchilla de fundición estampada combinada con un proceso modificado de inversión de fase asistida por atomización sin solvente. Este supera las limitaciones de los métodos utilizados anteriormente, como el micromoldeo por separación de fases (PSμM) y la litografía de impresión (IL), puesto que la separación de fases es inducida desde el lado del patrón y reducción en el tamaño de poro no es observada. Estudios previos para membranas TFC estampadas solo han logrado crear una capa superior de PA sobre soportes de UF con diseño con alturas en el rango de 160 nm a 5 μm, lo que limita las ventajas potenciales de tales membranas. Los soportes con patrones de s-NIPS pueden mejorar significativamente la baja permeabilidad intrínseca de tales membranas de NF / RO al producir soportes de UF con alturas de patrones más altas de hasta 180 μm. Por lo tanto, este estudio tiene como objetivo obtener una capa de PA de película delgada libre de defectos, sobre soportes con micro-patrones s-NIPS mediante polimerización interfacial (IP). Para lograr esto, se han explorado varios parámetros como por ejemplo el efecto de la concentración de los monómeros, el efecto de la altura del patrón, la eliminación del exceso de solución de monómero de los valles antes de IP, el efecto del soporte UF polimérico y la deposición de película delgada capa por capa. Se encontró que la membrana de TFC de 1, 2 y 3 capas podía alcanzar un máximo de aprox. 85, 96 y 97% de retención de $MgSO_4$, respectivamente, y una mayor permeabilidad. Además, se encontró que la IP asistida por centrifugado en 2 capas con 2% en peso de MPD y 0,1% en peso de concentración de TMC era óptima para soportes PSf_{500} (soportes de polisulfona preparados con una cuchilla de fundición con altura de patrón de 500 μm) con 94% de retención de $MgSO_4$ y una permeabilidad de 1,66 LMH / bar.

Table of Contents

List of Figures

List of Tables

List of Abbreviations and Symbols

TFC	Thin film composite
RO	Reverse osmosis
UF	Ultrafiltration
MF	Microfiltration
NF	Nanofiltration
IP	Interfacial polymerization
PSf	Polysulfone
PAN	Polyacrylonitrile
PI	Polyimide
PA	Polyamide
ΔP	Pressure gradient
ΔT	Temperature gradient
ΔC	Concentration gradient
ΔE	Electric potential gradient
C_f	Feed concentration
C_p	Permeate concentration
R	Retention
J	Flux
v_p	Permeate volume
A_m	Membrane area
t	Time
MWCO	Molecular weight cut-off
R_{tot}	Total resistance
R_f	Resistance due to fouling
R_{cp}	Resistance due to concentration polarization
R_m	Membrane resistance
TIPS	Temperature-induced phase separation
EIPS	Evaporation induced phase separation
VIPS	Vapour induced phase separation
NIPS	Non-solvent induced phase separation
PSμM	Phase separation micromolding
IL	Imprinting lithography
VIPSμM	Vapour-induced phase separation micromolding
s-NIPS	Non-solvent spray assisted phase inversion

X-PI	Cross-linked polyimide
PVP	Polyvinylpyrrolidone
PEG	Polyethene glycol
MPD	m-Phenylenediamine
TMC	1,3,5-Benzenetricarbonyl trichloride
NMP	N-methyl-2-pyrrolidone
DMSO	Dimethyl sulfoxide
THF	Tetrahydrofuran
TEA	Triethylamine
SDS	Sodium dodecyl sulfate
HDA	1,6-hexanediamine
DI	Deionised
RT	Room temperature
h-PAN	Hydrolysed PAN
CFD	Computational fluid dynamics
SEM	Scanning electron microscopy
FTIR	Fourier-transform infrared spectroscopy
LMH/bar	$L\ m^{-2}\ h^{-1}\ bar^{-1}$
XPS	X-ray photoelectron spectroscopy
AFM	Atomic force microscopy
TEM	Transmission electron microscopy
LBL	Layer by layer

1. Introduction and Objectives

1.1. Background

Membrane technology has made remarkable progress in the 21st century from an evident slow start in 1950s. Membrane-based processes have a clear edge over conventional separation processes due to its low cost, high energy efficiency, easy upscaleability and environmental sustainability. It has developed numerous applications in the field of agriculture, pharmacy, energetics, food technology, air protection and water purification [1]. In recent years, it has attracted the attention of chemists and engineers due to the selective transport of species and continuous efficient separation under mild operating conditions with relatively low energy consumption [2].

According to the United Nations world water development report 2020, global water use has grown by the factor of six in the last 100 years and continues to increase steadily at a rate of about 1 % per year because of the increasing population, change in consumption patterns, climate changes and economic development [3,4]. Membrane technology has emerged as the saviour in this regard and has been used extensively for wastewater treatment [5], water purification [6] and desalination [7]. Pressure driven membrane separation processes such as reverse osmosis (RO) and nanofiltration (NF) are state of the art techniques for desalination, seawater pre-treatment, water softening, wastewater reclamation and surface water purification [8]. Despite the significant progress achieved, there are few challenges which still needs attention and there is scope of advancement to meet the increasing demand for freshwater.

Membrane fouling caused by the unwanted deposition of foulants on membrane surface or/and into its pores is an unavoidable problem in membrane-based separation processes since they cause permeate flux decline and subsequently increase the operational cost [9,10]. Several attempts have been made to mitigate the membrane fouling which could be categorized mainly as physical, chemical and hydrodynamic methods. In physical methods, external forces such as membrane rotation [11], vibration [12] and electrophoresis [13] reduce the membrane fouling. Chemical methods include modification in membrane material and surface chemistry or application of chemical cleaning agents for fouling mitigation [14]. In hydrodynamic methods, fluid behaviour close to membrane surface is utilized to mitigate membrane fouling. Different ways such as turbulent promoter, feed spacer and patterned membranes have been applied to interfere with fluid behaviour near membrane surface [15,16]. Recent studies reveal that pattered membranes have great potential to enhance the state of the art membrane-based separation performance by giving higher fluxes without largely compromising the salt rejection

and providing higher fouling resistance [8,16,17]. However, there are still several challenges which hinder the widespread industrial application of patterned membrane for water treatment.

Polyamide (PA) thin-film composite (TFC) membranes are widely used in industries for pressure-driven RO and NF processes. Mostly, TFC ultra-thin selective layer is formed on porous support through interfacial polymerization (IP) of an amine monomer and an acyl chloride monomer. Rejection and permeability of the resulting TFC membranes strongly depend upon the morphology and structure of thin selective layer which depends on various other parameters such as concentration of monomers, IP reaction conditions and properties of the porous support [18]. Furthermore, the adhesion between the support layer and the selective layer is another important issue. Selective layer gets ruptured and delaminated under high pressure during filtration, resulting in low salt rejection [19]. Besides IP over patterned supports can be challenging due to the intrinsic crests and troughs, which can lead to the formation of cracks over the top layer, hence selection of pattern height and support material is also important [20].

1.2. Objectives

Several parameters must be considered in order to obtain a perfect micro-patterned TFC membrane for water treatment, some of them could be optimized through extensive literature review and others are achieved through experiments to meet the objectives

- Optimization of UF-patterned support: effect of different pattern heights of the supports, effect of different polymer i.e. PSf, PAN and cross-linked PI supports.
- Optimization of the IP method: effect of varying monomer composition, effect of layer by layer PA deposition.
- Study of obtained micro-patterned thin-film composite membranes for $MgSO_4$ rejection and permeance.

2. Literature Review

In this chapter, an extensive literature review of the state-of-the-art will be carried out in order to identify the existing research gaps. It would cover a general introduction to membrane technology, fouling of membranes, patterned membranes and their different synthesis procedures, TFC membranes, their synthesis procedures and applications.

2.1. Membrane technology

Membrane technology covers several separation processes of components through a selective mass transport using a semipermeable barrier called membrane. It restricts the mass transport of one component and favours the other under different driving forces such as gradient of pressure, temperature, concentration or electric potential (*Fig. 1*). Component of the feed stream which passes through the membrane is called permeate, while the retained components stream is called retentate [21].

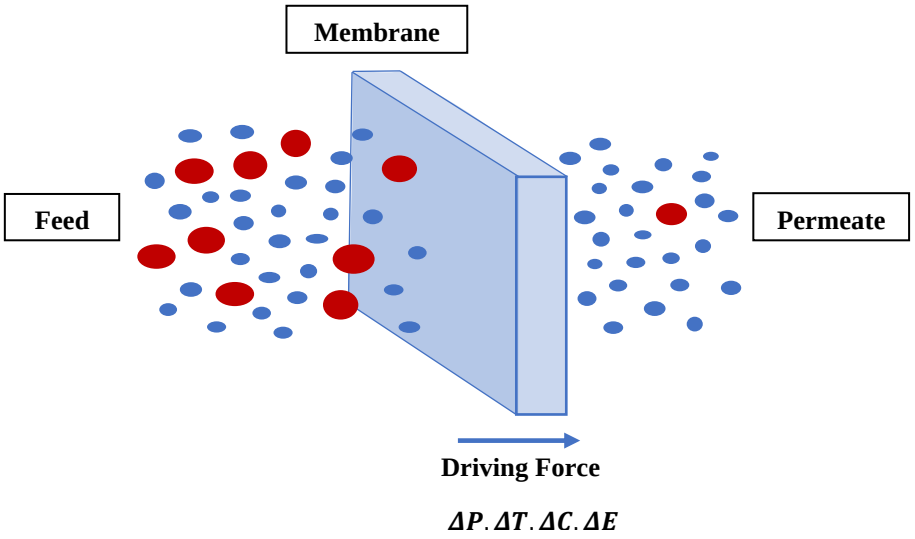

Fig. 1. *Schematic representation of the basic membrane separation process. Driving force separates the feed stream which is a mixture of components into permeate and retentate*

Separation processes play an important role in various industries. For instance, it contributes ca. 40-70% of the operating and capital costs in pharmaceutical and chemical industries [22]. Membrane technology is the key solution to a very large number of separation needs, it performs a variety of separation from the molecular level up to the scale where particles are visible with naked eyes. Additionally, it could be applied as a continuous process, also in combination with other separation technique if required. These factors make membrane-based separation advantageous over conventional techniques such as distillation, extraction, crystallization and adsorption. In a wide range of applications, membrane processes based on different driving forces (*Fig. 1*) are used. For water treatment, generally pressure-driven membrane processes such as microfiltration (MF), ultrafiltration (UF), nanofiltration (NF), reverse osmosis (RO) are utilized.

2.1.1. Pressure-driven membrane processes

Pressure-driven membrane separation processes represent a wide range of diverse applications from a very common coffee filter to a huge water desalination plants producing potable water for millions. Driving force in the form of pressure gradient causes the separation of feed into

permeate and retentate in generally classified pressure-driven membrane processes: MF, UF, NF and RO. Applied pressure as driving force, typical permeance, morphology of the selective layer, and size of the separated component can be used to distinguish these processes (*Table 1*).

***Table 1**. Classification of pressure-driven membrane processes [21,23]*

Process	Pressure (bar)	Permeance (l/(m^2.h.bar))	Membrane morphology	Pore size (nm)	Retained components
MF	0.1 - 2.0	>50	Porous	20 - 10000	Particles, Clays, Bacteria
UF	1.0 10	10 - 50	Porous	1 - 50	Virus, Macromolecules (Polysaccharides)
NF	5.0 - 35	1.4 - 12	Porous/Dense	< 2	Low MW-components (Polyvalent salts)
RO	10 - 150	0.05 - 1.4	Dense	No pores	Monovalent salts

The membrane efficiency or performance is evaluated by two parameters: retention or selectivity and the permeate flux (permeance or permeability). Selectivity of membrane towards a component is generally expressed by retention (R) in terms of solute concentration the feed (C_f) and solute concentration in the permeate (C_p) (*Eq. 1*). Flux (J) is the amount of permeate that migrates through per unit membrane area and time (*Eq. 2*). Normalised flux per unit pressure is the permeance while permeability is an intrinsic property of membrane obtained by diving the permanence by the thickness of membrane [21,24].

$$Retention\ (R) = \frac{c_f - c_p}{c_f} = 1 - \frac{c_p}{c_f}$$

Eq. 1: Retention (R) in terms of solute concentration in feed (c_f) and permeate (c_p)

$$Flux\ (J) = \frac{v_p}{A_m t}$$

Eq. 2: Flux (J) in terms of permeate volume (v_p), membrane area (A_m) and time (t)

Often, membranes are characterized by the concept of molecular weight cut-off (MWCO) which is defined as the molecular weight of the solute which corresponds to the 90 % retention [24]. A good membrane should have high permeate flux with high retention, long term stability

under diverse operating conditions, minimal fouling and an economically suitable defect-free production.

2.1.2. Membrane fouling

Membrane fouling is caused by the unwanted deposition of foulants on the membrane surface or/and into its pores, which reduces the permeate flux and increases the operational cost. Additionally, concentration polarization can also cause flux reduction, and is occurred due to the higher concentration of feed near membrane surface of the feed side. The total resistance to the permeate flow (R_{tot}) combines the intrinsic membrane resistance along with resistances due to concentration polarization and membrane fouling, which is incorporated into the modified Darcy´s law to obtain the flux (*Eq. 3*).

$$J = \frac{\Delta P - \Delta \pi}{\eta \cdot R_{tot}}$$

Eq. 3: Modified Darcy´s law with R_{tot}

Where R_{tot} is the sum of resistances due to fouling (R_f), concentration polarization (R_{cp}), and constant membrane resistance (R_m). Under the steady-state conditions, concentration polarization gives almost a constant resistance to mass transport while fouling increases with time causing a severe decline in flux (*Fig. 2*). Therefore, fouling is a critical issue to control for better membrane performance [25].

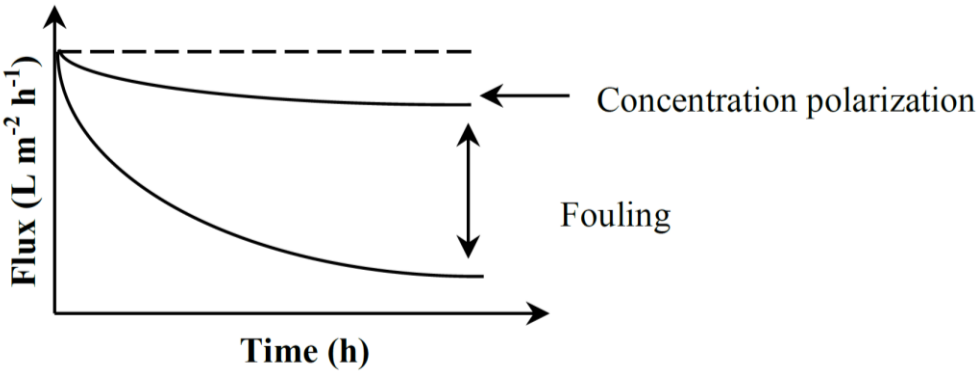

Fig. 2. *Effect of concentration polarization and membrane fouling over flux with filtration time[25]*

Several techniques for membrane fouling mitigation including physical cleaning, chemical treatment and hydrodynamics variation have been used. Several reports [8,16,17,26–29] have suggested higher fouling resistance for patterned membranes.

2.2. Patterned membrane

Pattern or corrugation on the membrane surface changes the hydrodynamics of fluid near the surface of membrane by generating the eddies which can reduce the phenomenon of

concentration polarization and cause diffusion of foulants away from the surface [30–33]. Furthermore, surface pattern prevents the deposition of foulants into the valleys if it is bigger than the valley size or in case of similar size by changing the crystallization entropy [34]. Local mixing near the membrane surface due to pattern causes turbulence which reduces the requirement of liner velocity causing smaller pressure drop along the module (*Fig. 3*) [35].

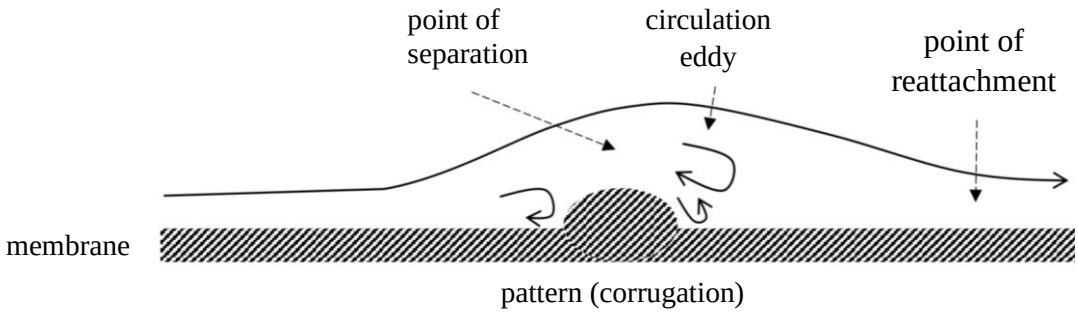

Fig. 3. *Streamline for flow over a patterned membrane; adapted from [36]*

Indeed, patterned membrane has great potential to enhance the performance of currently used flat membranes for water treatment. However, several synthesis procedures have been reported in the literature in order to achieve patterned surfaces of the membranes. A comprehensive analysis of all those methods is provided in the next section.

2.2.1. Synthesis procedures for patterned membranes

Phase separation is one of the most used processes to produce porous polymeric membranes [37]. This technique involves controlled precipitation of a casted polymeric solution into a porous membrane. During the process, a thermodynamically stable polymer solution separates into two phases: polymer-rich phase which solidifies to produce the matrix of the membrane and the polymer-lean phase which produces the pores in the membrane. This phase separation can be induced by several techniques: by lowering the temperature through so-called temperature-induced phase separation (TIPS), by evaporating the volatile solvent through evaporation induced phase separation (EIPS), by contacting the cast solution with a vapour phase of non-solvent through vapour induced phase separation (VIPS) and foremost by immersing the cast polymer solution into a non-solvent bath called non-solvent induced phase separation (NIPS) [37].

Methods used for producing patterned membranes can be classified into two main categories: template-based synthesis and direct printing. Template-based synthesis methods include phase separation micromolding (PSμM), imprinting lithography (IL) and use of smart spinnerets for pattern membrane production (*Fig. 4*). In PSμM, phase separation is induced through NIPS or

VIPS after casting the polymer solution over a patterned mold [16,38]. Imprinting lithography involves stamping or imprinting of mold over a prepared membrane [17,39]. Direct printing method such as 3D-printing [40] and inkjet printing [26] have recently been explored to produce patterned membranes.

PSμM has a major limitation that the phase separation is induced from the flat side, which creates pore size gradient and forming the selective layer on the non-patterned side of the membrane [41]. Therefore, the use of non-solvent permeable mold for vapour-induced phase separation micromolding (VIPSμM) was introduced to produce patterned membrane with isotropic pore size distribution [41]. This is somewhat a complex approach due to challenging mass transport of non-solvent/solvent through the porous mold. Whereas, in case of IL an already prepared membrane is imprinted by mold using pressure and temperature. Application of proper temperature is quite challenging since it must be below the glass transition temperature of membrane material and it should not induce pore collapse and affect the pore size and permeance [39]. Smart spinneret is clearly not suitable for our purpose is to produce patterned flat sheet porous support for TFC membrane. Furthermore, 3D-printing and inkjet printing could be used only with limited polymers and it gives moderate resolution and poor fidelity [42].

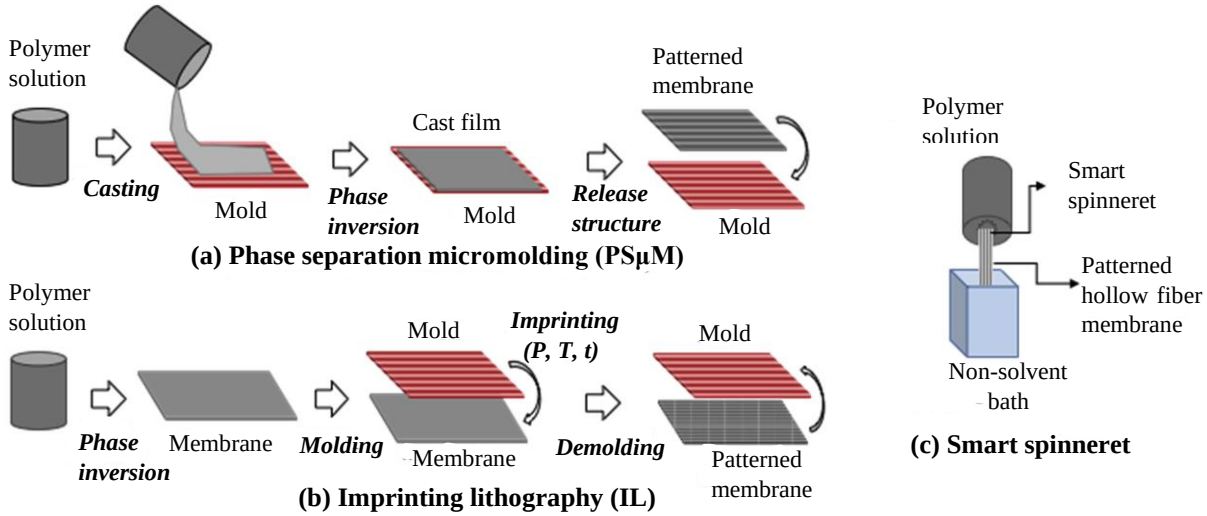

Fig. 4. *Template-based synthesis methods for patterned membrane (a) phase separation micromolding (PSμM) (b) imprinting lithography (IL) (c) smart spinneret combined with phase separation; adapted from [43]*

Recently, a one-step method to produce flat-sheet patterned membrane has been developed in prof. Vankelecom's laboratory in KU Leuven [43]. In this method, a patterned casting knife and a modified non-solvent spray assisted phase inversion process is used and referred as s-NIPS (*Fig. 5*). After pouring the polymer solution on the glass support, the patterned casting

knife induces the desired pattern over the top surface while casting. Non-solvent is sprayed simultaneously, following the movement of casting knife to prevent further flow and solidify the polymer (*Fig. 5 b*). Detailed spray control panel for s-NIPS included in the appendix (*Fig. A-1, A-2*).

Unlike PSμM in the case of this one-step method (s-NIPS), phase separation occurs from the side of patterned surface, resulting in desired top layer with higher surface area. There is no need for pressure and temperature application like IL. Additionally, it could be used for all the polymers for which phase separation is suitable. This way, s-NIPS overcomes all the limitations of previously mentioned methods and would be well suitable to produce UF support for our TFC membranes. A brief description of TFC membranes, analysis of effects of supports and interfacial polymerization condition is given in the next section.

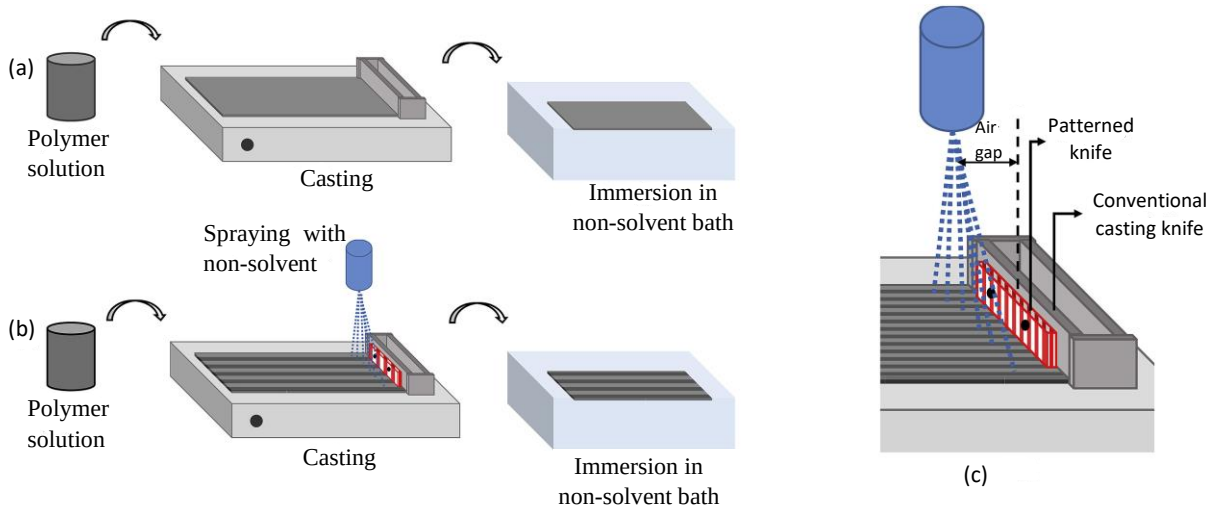

Fig. 5. *Patterned membrane preparation (a) conventional NIPS, (b) application of patterned casting knife with modified spray-assisted phase separation (s-NIPS), (c) detailed schematic representation of s-NIPS set up; adapted from [43]*

2.3. Thin film composite (TFC) membranes

TFC membranes are asymmetric membranes, comprised of a dense ultra-thin top layer over a porous UF support. Generally, both the selective layer and porous support are prepared separately which enables them to be optimized independently to obtain high-performance RO and NF membranes. The top selective layer has a very low thickness in the range of 10-200 nm due to which it needs support to provide the mechanical strength, though it is considered that only top selective layer determines the salt rejection and water permeation [19]. The porous support is generally fabricated via phase separation method.

The objective of this study is to enhance the permeability and fouling resistance of TFC membranes by making it on patterned support which would be obtained by s-NIPS. The top selective layer could be produced in many different ways, but the most used method is interfacial polymerization (IP). Other methods include spin or dip coating, plasma-initiated polymerization, photo grafting, and electron beam irradiations [44]. IP is a widely used method for production of commercial TFC NF and RO membranes for water treatment [45]. In this study, we would be using IP to make TFC selective layer over patterned porous support.

2.3.1. Effect of support

It is believed that only the top selective layer determines the selectivity and permeability of TFC membranes yet the adhesion between the thin layer and support is important. The selective layer could be delaminated under operating pressure due to inadequate adhesion causing bulk flow and poor membrane rejection. Properties of support material influence the IP and hence the selective layer properties. Also, unfavourable interaction due to different hydrophilicity of two layers promotes the delamination of the active layer from support. Hence, we would be studying the effect of different support materials i.e. polysulfone (PSf), polyacrylonitrile (PAN) and cross-linked polyimide (X-PI). Furthermore, additives such as polyvinylpyrrolidone (PVP) and polyethene glycol (PEG) when added into the casting solution, increases the porosity and hydrophilicity of the membranes [46].

2.3.2. Interfacial Polymerization (IP)

Development of interfacial polymerization (IP) as a technique to prepare composite membranes by *Cadotte* was a major breakthrough [47]. IP has been developed as a well-established method for production of selective top layer of TFC NF and RO membranes for water treatment. By far, TFC membrane with a selective top layer of PA is most common for RO and NF membranes.

Interfacial polymerization occurs through a simple mechanism, in-situ polymerization reaction occurs at the interface of two immiscible solvents containing an amine and an acid halide monomer, which results in an ultrathin selective barrier over porous UF support. Polymeric porous support is saturated in the solution containing amine monomer. Excess solutions from the surface of flat support are generally removed by rubber wiper or an air knife. However, removal of excess amine could be challenging in case of the patterned membranes, which would be optimised through various experiments in this study. After removing the excess solution, support saturated with amine monomer is contacted with the immiscible organic solvent containing acid halide. Each monomer reacts at the interface of two immiscible

solutions to quickly generate a thin layer on the surface of support thus making a TFC membrane [48]. Different combination of amine and acid halide monomers have been tried for IP, so far m-phenylenediamine (MPD) as the amine and 1,3,5-Benzenetricarbonyl trichloride (TMC) as acid halide monomer gives promising result for several applications [49–51]. Therefore, for our objective to create a defect-free thin film layer on pattern support we would use MPD and TMC monomers (*Fig.6*).

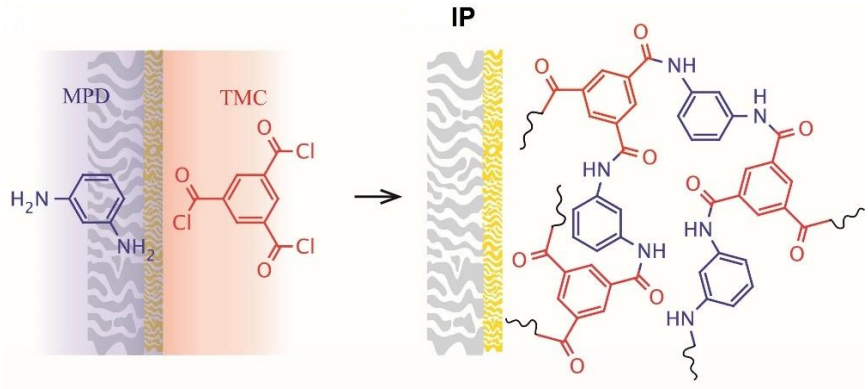

Fig. 6. *Schematic representation of fabrication of TFC membrane with PA top layer through IP [51]*

2.3.2.1. Additives

Many additives have been added to the reacting solutions during membrane synthesis through IP. Components such as polyethene glycol or surfactant like sodium dodecyl sulfate increase the wettability of pores in the support. The aqueous solution containing amine monomer can thus penetrate easily into the smaller pores enhancing the extent of IP [52]. Bases such as sodium hydroxide and triethylamine when added, remove hydrogen halides which accelerate the reaction between amine and acid halide [53].

2.3.2.2. Polymerization Parameters

TFC membrane performance depends upon several parameters which could be adjusted during IP. Generally, higher monomer concentrations and prolonged reaction times support improved polymerization giving a thicker top selective layer [54]. Thicker selective layer gives higher selectivity but reduces the permeance. Type of solvents used for both monomers also affects the performance of TFC membrane, its density, surface tension, viscosity and insolubility affect the diffusion of monomer affecting the properties of the top layer. Furthermore, temperature, humidity and atmosphere also affect the polymerization reaction. At higher temperature, due to higher diffusion molecules collide vigorously hence improve polymerization [55].

2.3.2.3. Post-treatments

Cross-linking of top PA layer and residual solvent removal is achieved through curing step at increased temperature. Higher temperature or longer curing time enhance the degree of

crosslinking and density of TFC membrane. However, prolonged curing or too high temperature could damage the membrane resulting in inferior selectivity [55].

2.4. State-of-the-art and scope

Patterned TFC composite membranes have been produced successfully through different processes and resulted in RO-like selectivity and permeability [16,17,26,41,42,56,57]. However, in all these studies patterned supports were obtained through template-based method or modified VIPSμM. Patterned supports obtained through these methods have major limitation such as pore size gradient caused by phase separation induction from the flat side of the membrane and pore size reduction. It has been established through mathematical modelling and experimental studies that the higher pattern due to increased hydrodynamics and effective surface area reduces mass deposit and increases water flux in turn [27,35]. Therefore, it is expected that newly developed patterned membrane synthesis process s-NIPS [43] (explained in section 2.2.1.) would give several advantages over any other previously reported method. Previous studies for patterned TFC membranes have only managed to create a polyamide (PA) top layer above patterned UF supports with heights in the range of 160 nm to 5 μm and still suffer from low permeate fluxes. Hence, limiting the potential advantages of such membranes [41,58]. s-NIPS patterned supports can significantly enhance the intrinsic low permeance of such NF/RO membranes by producing UF supports with higher pattern heights up to 180 μm. However, higher pattern makes it difficult to obtain a defect-free thin selective layer because of higher crests and troughs. Hence, this study aims to obtain a defect-free thin film PA layer over s-NIPS micro-patterned supports. In order to achieve this, several parameters have been explored including effect of monomer concentrations, effect of pattern height, removal of excess monomer solution from the valleys before IP and selection of optimum UF polymer support.

3. Experimental Section

3.1. Materials

Polymers, polysulfone (PSf, Udel 1700, powder, MW: 81,000 Da), polyacrylonitrile (PAN, powder, MW: 150,000 Da) and polyimide (PI, Matrimid 9725, powder) were obtained from Solvay, Sigma-Aldrich and Huntsman respectively. All the polymers were dried overnight in an oven at 100 °C before use. Solvents, N-methyl-2-pyrrolidone or 1-methyl-2-pyrrolidone (NMP, liquid, 99%, extra pure), dimethyl sulfoxide (DMSO, liquid, 99%, extra pure) and tetrahydrofuran (THF, liquid, 99.9%) were supplied by Acros Organics, Alfa Aesar and Sigma-Aldrich respectively. Monomers, 1,3,5-benzene tricarbonyl trichloride or trimesoyl chloride

(TMC, powder, 98%) and 1,3-phenylenediamine or m-phenylenediamine (MPD, flakes, 99%) were acquired from Sigma-Aldrich. Additives, polyethylene glycol (PEG, MW: 10,000 Da), triethylamine (TEA, liquid, 99.7%, extra pure) and sodium dodecyl sulfate (SDS, powder) were obtained from Alfa Aesar, Acros Organics and Sigma-Aldrich respectively. 1,6-hexanediamine (HDA, solid), n-hexane (liquid, extra pure 99%) and acetone (lab grade, 99% pure) were provided by Acros Organics. Magnesium sulfate ($MgSO_4$, MW: 120 Da) and Sodium hydroxide (NaOH, pellets) were acquired from Honeywell. Milli-Q (MQ) water was obtained from in house water purification system (Synergy ®) and deionised (DI) water was supplied by our lab's piping system both at room temperature (RT, 25 °C). All the chemicals were used as they were supplied, without any further purification.

3.2. Fabrication of patterned supports

Micro-patterned ultrafiltration (UF) supports based on three polymers i.e. PSf, PAN and crosslinked PI (X-PI) were produced with three different pattern heights of 500, 700 and 900 µm. For all supports, the same casting procedure (s-NIPS) with different casting knives was followed, though the composition of polymer solution and solvents were different in each case.

3.2.1. Casting solution preparation

Two PSf solutions, one with additive PEG and one without it for conventional flat TFC membranes were prepared by adding the required amount of oven-dried PSf into NMP (*Table 2*). Hydrophilic polymer PEG was added into the solution to enhance the wettability of porous support as well as to enhance the viscosity of polymer solution which helps in pattern formation. The overall composition of the polymer solutions was inspired from the study reported elsewhere [59].

***Table 2**. Composition casting solutions for PSf supports*

UF support	PSf (wt%)	PEG (wt%)	NMP (wt%)
Flat PSf	18	NA	82
Patterned PSf + reference flat	18	22	60

For PAN supports, two solutions containing 15 wt% and 17 wt% PAN in DMSO were prepared (*Table 3*). Thanks to the polar nature of PAN, addition of PEG was not required to enhance the wettability and viscosity of solution was high enough for retaining the patterns.

***Table 3**. Composition of casting solutions for PAN supports*

UF support	PAN (wt%)	DMSO (wt%)
PAN 15 wt%	15	85
PAN 17 wt%	17	83

In the case of PI support, casting solution with 24 wt% PI in 3:1 mixture of NMP and THF were prepared. For all the casting solutions after adding polymers into the solvent in required proportions, the mixture was stirred at RT for 24 h. Subsequently, polymer solutions were degassed overnight to avoid any defect in membrane due to air bubbles. The casting solution was always stored in an airtight glass bottle with lid properly sealed with parafilm to prevent composition change due to solvent evaporation.

3.2.2. Micro-patterned supports casting via s-NIPS

Patterned supports from all the casting solutions mentioned above i.e. PSf, PAN and PI were obtained using s-NIPS. Patterned casting knives were prepared with photopolymerization based 3D-printing using Objet30 Prime printer (Stratasys Ltd, Eden Prairie, USA) in FabLab (KU Leuven) and VeroWhitePlusTM RGD835 (Stratasys Ltd, Eden Prairie, USA) was used as resin material. Patterned knives having different pattern heights (500, 700 and 900 μm) were attached to a regular aluminium knife. Schematic front view of casting knife attached with pattern knife and obtained membrane is shown (*Fig. 7 (a) and (b)*, respectively).

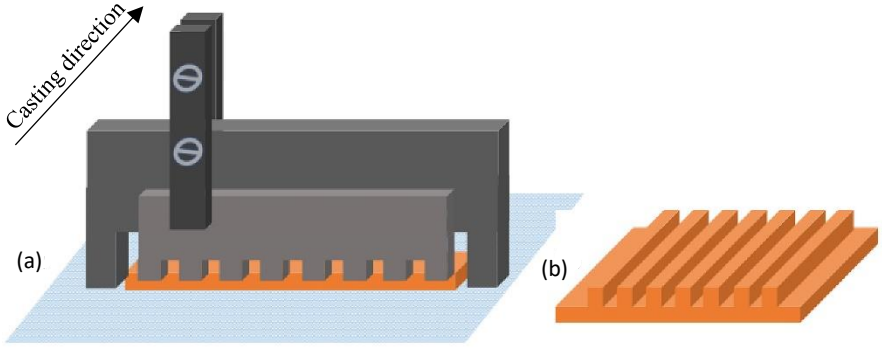

***Fig. 7.** (a) Schematic front view of casting knife attached with patterned casting knife (b) the obtained membrane*

In the first step of casting, completely degassed polymer solution (confirmed by visual inspection) was poured into the gap of aluminium casting knife which was placed over a glass support. The casting thickness i.e. distance between patterned casting surface and support glass was always kept as 200 μm. Once the polymer solution completely spread throughout the gap of casting knife, membrane was casted over the glass support using automatic film casting

machine (Braive Instruments, Belgium) (*Fig. A-2*) combined with automated non-solvent spraying system. Briefly, the gap in the casting knife was filled with polymer solution, then it was moved at a defined casting speed followed immediately by an automatic spray of non-solvent water and finally immersion in non-solvent (DI water at room temperature) bath (*Fig. 8*). The non-solvent spray system used was an AutoJet® (2008) + control panel manufactured by Spraying Systems Co. (USA) [60].

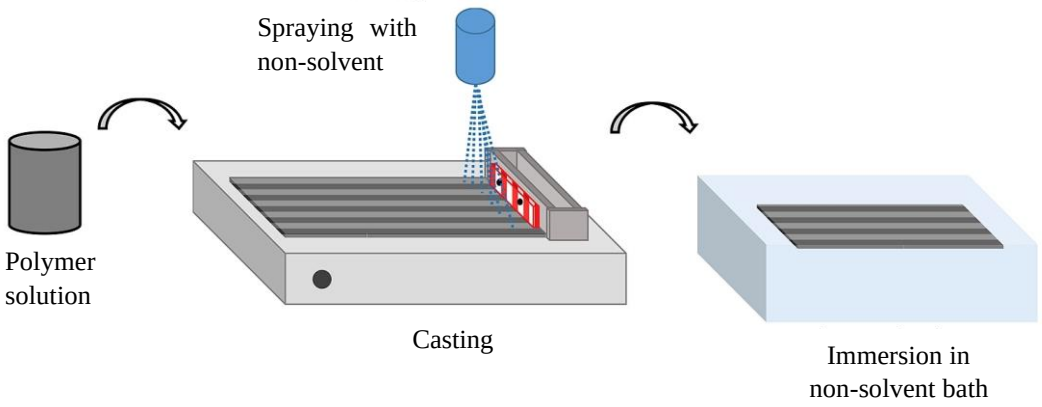

Fig. 8. *Patterned membrane preparation via s-NIPS using spraying and patterned casting knives*

During casting, non-solvent reservoir was filled with DI water at RT and kept under pressure of 2 bar using compressed N_2 and the distance between spraying device (PulsaJet®) outlet and casted membrane was kept 15 cm (*Fig. A-1, A-2*). This spraying distance and other casting parameters such as casting speed and materials of patterned casting knife were optimized by M. Dierick [61] and Marbelia *et al.* [43] and it gave 12 cm wide coverage over the membrane surface. Given the time frame of the thesis, casting knives with pattern height ranging from 500 to 900 µm were selected, therefore PAN supports were prepared using 900 µm and 700 µm, PSf using 500 µm and 700 µm and PI only with 700 µm. For all PAN supports, presence of C ≡ N bond gave possibility for surface treatment, it was hydrolysed by treatment with 10 wt % NaOH at 50 °C for 1 h under continuous stirring [62]. h-PAN supports enabled the MPD to be chemically bonded with the obtained carboxyl group resulting in enhanced adhesion of polyamide selective layer with the UF PAN supports (*Fig. 9*). The PI supports were post crosslinked using 1,6-hexanediamine (HDA) to improve the chemical stability. The membranes were first wiped with a paper towel to remove excess water and then immersed in gently stirred 1 w/v % HDA solution in MQ water for 1 h in a completely covered container to avoid any photodegradation. Flat PSf and PSf/PEG supports were prepared using conventional flat aluminium casting knife via the conventional phase inversion technique [63]. In all cases, support membranes were rinsed and stored in DI water until further use.

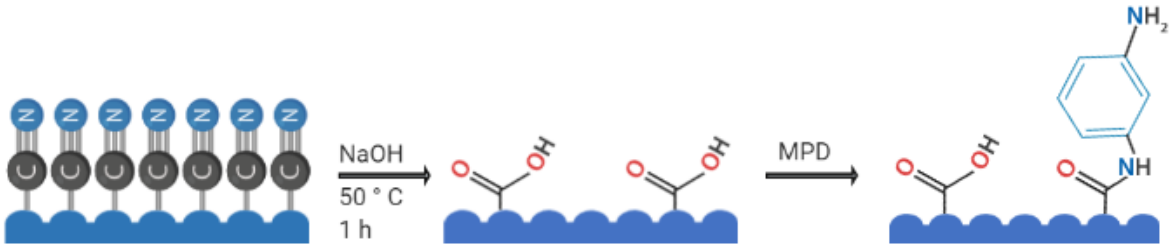

Fig. 9. *Schematic representation of surface treatment of PAN supports, which enabled MPD to be chemically bonded with support resulting in improved adhesion between selective layer and UF support*

3.3. Interfacial polymerization (IP)

Thin film composite (TFC) membranes over the UF supports were obtained by interfacial polymerization (IP) of monomers TMC and MPD (*Fig. A-3*). Concentration of monomers, extra monomer removal from the surface and presence of other additives in the monomer solution highly influence the performance of the TFC membranes. In this study, concentration of TMC and additives added were kept same for all membranes and was adapted from the studies reported elsewhere [64,65]. Aqueous solutions of varying MPD concentrations with 0.1wt% SDS and 2 wt% TEA were prepared in MQ water. 200 mL solutions with MPD concentrations of 0.5 wt%, 1 wt%, 1.5 wt%, 2 wt% and 2.5 wt% were prepared in a completely covered container to avoid any photodegradation. TEA was added to improve the extent of IP by removing HCl formed during the polymerization of TMC and MPD. Theoretically, TEA could also react with TMC and compete with MPD, hence hindering the IP. However, the rate of reaction of TMC with MPD is way higher than TEA. SDS was added to improve the wettability of the pores of the supports. TMC solution was prepared with 0.1 w/v % in n-hexane.

Keeping in view the preliminary study carried out by Ayesha Ilyas [66] for different methods to remove the excess MPD over the supports. Two different methods were further investigated to remove the excess MPD combined with repetition of more than 1 IP cycles in order to cover any defect formation due to higher pattern heights. Firstly, owing to the high solubility of MPD in acetone and subsequent quick drying, washing the supports with acetone was added as a step to remove excess MPD. Patterned PAN supports were first soaked in aq. MDP solution (2.5 wt %) for 30 min at RT under continuous stirring. After that, the supports were rinsed with 5 mL acetone to remove the excess MPD and was kept vertical for 2 min for complete drying. Afterwards, a lag time of 2 min was added prior to adding 5 mL TMC solution for 60 s. In house developed IP setup was used, in which membranes were placed over a metal plate and clamped with pressure holders to prevent any leakage (*Fig. A-4*). Finally, a thin layer of PA

was obtained over the patterned UF support. This marks the completion of one cycle and several layers of such thin film were obtained by repeating the modified IP steps (*Fig. 10*). 1, 3 and 5 PA layers were obtained using the above-mentioned process on PAN supports with 900 μm patterned height (*Table 4).*

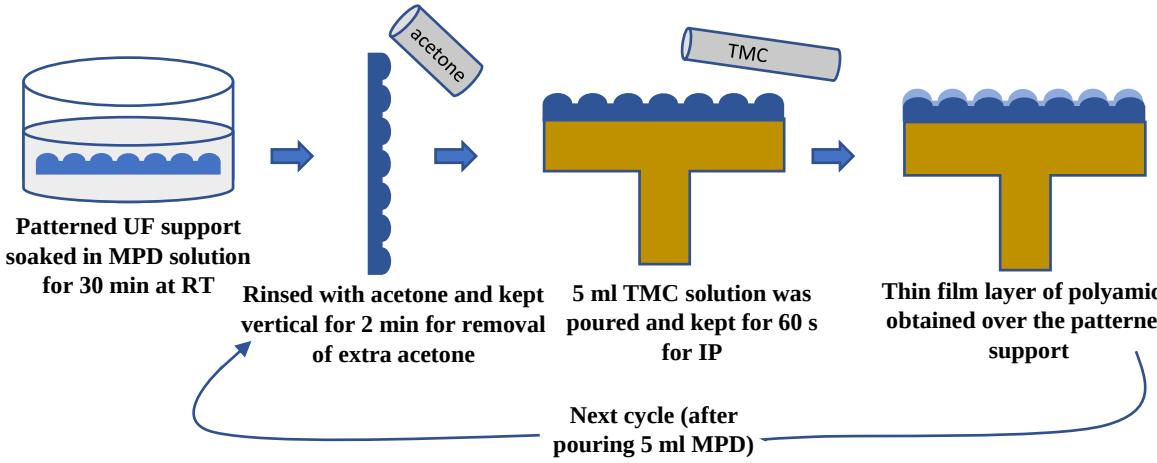

Fig. 10. *Schematic representation of interfacial polymerization in which extra MPD was removed by rinsing with acetone and 2 min lag time*

Table 4*. TFC membranes prepared with PAN supports with pattern height of 900 μm*

UF support (900 μm)	Membrane name*	Number of PA layers
PAN	PAN_{900}^{1L}	1
	PAN_{900}^{3L}	3
	PAN_{900}^{5L}	5

**In membrane name, the digit before L represents number of PA layers in TFC membranes, 900 represents the pattern height (μm) of casting knife used.*

For the second method, removal of the excess MPD was carried out via drying using the spin-coater. In order to further optimize the performance of the membranes, MPD solutions with different concentrations (0.5, 1, 1.5, 2 and 2.5 wt%) were used keeping the TMC concentration same as 0.1 wt%. Unreacted TMC after IP was also removed by spin-drying the membrane. PSf supports with two pattern heights 500 and 700 μm were used and 1, 2 and 3 layers of selective PA were created on each kind of supports by IP using 5 different MPD concentrations (*Table 5*). In the first step, supports were soaked in above stated MPD solution for 30 min at RT under continuous stirring like in the previous technique. Then MPD soaked membrane was placed over spin rotor and rotated at 700 rpm for 2 min to remove extra MPD from the valleys. After that, 5 mL TMC solution was poured over the membrane and kept still for 60 s to carry out IP and unreacted TMC was removed by rotating it again at 700 rpm for 2 min, which marks the completion of one cycle. The above-mentioned steps were repeated for further deposition

of another IP layer following the pouring of 5 mL MPD solution and its drying at 700 rpm for 2 min (*Fig. 11*). Complete spin rotor setup used in this study is included in the appendix (*Fig. A-5*).

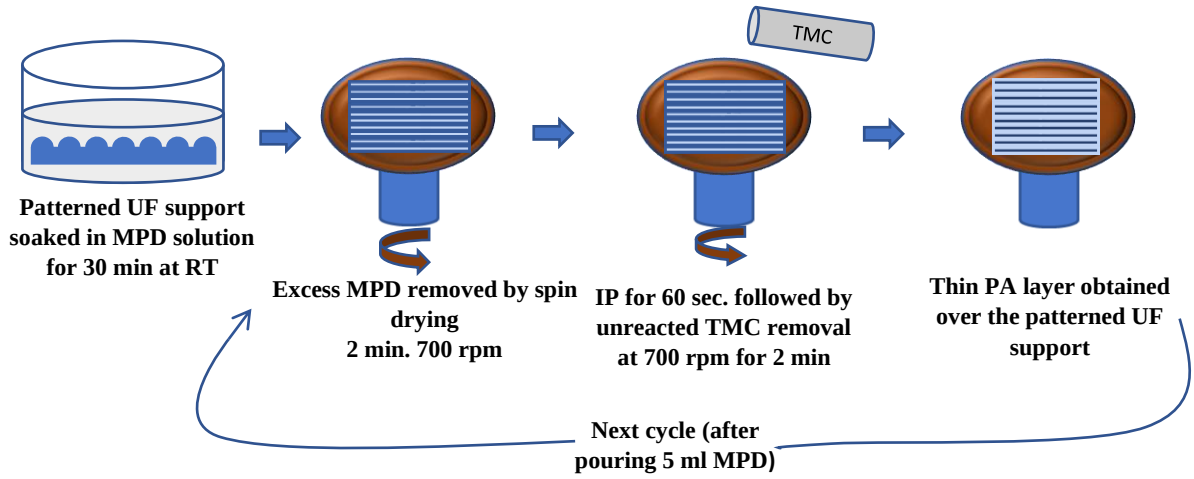

Fig. 11. *Schematic representation of interfacial polymerization in which extra MPD from valleys of UF supports was removed by spin drying and cycles followed to obtain 1, 2 and 3 layers of PA*

Table 5*. TFC membranes prepared with PSf, PAN and X-linked PI supports with pattern height of 500 and 700 µm using 2nd technique of IP*

UF support	Membrane name*	MPD concentration (wt %)	Number of PA layers
PSf (500 µm)	$PSf_{500}^{0.5\_1L}$	0.5	1
	$PSf_{500}^{0.5\_2L}$	0.5	2
	$PSf_{500}^{0.5\_3L}$	0.5	3
	$PSf_{500}^{1\_1L}$	1	1
	$PSf_{500}^{1\_2L}$	1	2
PSf (700 µm)	$PSf_{700}^{0.5\_1L}$	0.5	1
	$PSf_{700}^{1\_2L}$	0.5	2
	$PSf_{700}^{0.5\_3L}$	0.5	3
PAN (500 µm)	$h-PAN_{500}^{2.5\_3L}$	2.5	3
X-PI (500 µm)	$X-PI_{500}^{2.5\_3L}$	2.5	3

**TFC membranes were obtained over UF supports using MPD solutions with 5 different concentrations, here only few of them are mentioned, complete table in appendix (Table A-1). The digit before L in the superscript represents number of PA layers, while the first part of the superscript represents concentration of MPD used. 700 and 500 in subscript represents the pattern height (µm) of casting knife used.*

Flat TFC membranes over PSf and PSf/PEG supports were prepared using conventional interfacial polymerization technique reported elsewhere [63]. All membranes post IP were

heat-treated for further crosslinking at 70 °C for 2 min. Prepared TFC membranes were stored in a plastic bag until they were used for the filtration test.

3.4. Computational fluid dynamics (CFD) analysis

Cross-section model of the patterned membrane was developed using COMSOL Multiphysics 5.4 with corresponding pattern height. Velocity and shear stress profiles were obtained for feed at an angle of 90° with respect to membrane pattern. Further, it was compared with literature to validate its effect over membrane fouling. However, the experimental study of pattern's effect on membrane fouling still needs further research and was out of the scope of this thesis.

3.5. Membrane characterization and performance

3.5.1. Scanning electron microscopy (SEM)

SEM (SEM JEOL JSM-6010LV JEOL) was used to study the surface morphology, pattern height and cross-section of the patterned membranes. Surface images were obtained to investigate the typical ridge-valley morphology of PA top layer and the presence of any defects in the selective layer, while cross-section images could reveal the pattern height and the thickness of the top layer formed. It was important to know up to which pattern height thin film layer could follow the pattern of support without any defects. Membrane cross-sections were prepared carefully after immersion in the liquid N_2 and samples for surface analysis were obtained by cutting the membranes using scissors. Further, samples were coated with Au/Pd layer using Auto fine coater (JFC-1300).

3.5.2. Fourier-transform infrared spectroscopy (FTIR)

Attenuated total reflection Fourier-transform infrared spectroscopy (ATR-FTIR) was used to confirm the formation of PA selective layer over the patterned UF support. FTIR spectrometer (Bruker ALPHA-P) with ATR crystal was used to collect absorption peaks of dried membrane samples in the wavelength range of 400 to 4000 cm^{-1}. Formation of thin film PA layer was confirmed by comparing the absorption spectra of UF supports underwent IP with the support without any layer.

3.5.3. Membrane performance

To investigate the membrane performance for rejection and permeance, a high-throughput pressure-driven dead-end filtration set-up was used. The set-up is designed in such a way that 16 membrane samples with 20 mm diameter could be tested at the same time under the same operating conditions (*Fig. A-6*). Filtration test for all membrane coupons were done at 15 bar. Prior to filtration, membranes samples were cut into 20 mm circular coupons and placed on the porous metal plates which was covered with non-woven support. On the top of the coupons, an

o-ring made of rubber was placed to prevent any leakage. Because of this o-ring, the active diameter of membrane coupons involved in filtration decreased to 14 mm. Therefore, for permeance calculation surface area corresponding to diameter 14 mm was used. After complete installation, filtration set-up was pressurised to the operating pressure of 15 bar and membrane coupons were compacted for 2 h with water as the feed. After that, feed was changed to 2g/L $MgSO_4$ (120 Da) to study its rejection and permeance. Permeate was collected from each membrane coupon in glass vials which were pre-weighted. Using the mass difference of empty vials and permeate filled vials, permeance was calculated by using *Eq. 4*.

$$Permeance = \frac{\frac{(m_1 - m_0)[g]}{\rho_w[{}^{g}/_{L}]}}{A[m^2] * \Delta t[h] * P\ [bar]}$$

Eq. 4. Equation used for permeance calculation

where m_1 (g) is the mass of glass vial with permeate, m_0 (g) is the mass of same glass vial when it was empty. ρ_w is the density of water in g/L, A is active membrane surface area in m^2, Δt (h) is time of permeate collection and P (bar) is the applied pressure. Salt concentration of permeate collected from each membrane coupons was determined by measuring the conductivity of the sample and was used for retention calculation (*Eq. 1*).

3.5.4. Conductivity meter

A multi-parameter analyser was used to measure the conductivity of $MgSO_4$ solutions at different known concentration to draw the concentration calibration curve (*Fig. A-7*), the relation between conductivity and concentration was obtained from that curve (*Eq. 5*). Then the conductivity of permeates was obtained using the same device which was used in *Eq. 5* to obtain the $MgSO_4$ concentration in them.

$$Concentration\ ({}^{g}/_{L}) = \frac{Conductivity\ \left(\frac{\mu S}{cm}\right) - 92.55}{959.7}$$

Eq. 5. $MgSO_4$ concentration in terms of conductivity

4. Results and Discussion

This section describes the systematic investigation of IP over the patterned supports. Permeance and retention results for various IP and support parameters are given. The synthesized membranes were characterized via SEM and FTIR. Furthermore, the fluid hydrodynamics over the patterned membrane is analysed to investigate the effect on membrane fouling.

4.1. Effect of excess MPD removal by acetone rinsing

Various methods of excess MPD removal before IP including rubber wipes, lag time, paper wipes, cyclohexane rinsing and air knife were examined by Ayesha Ilyas [66]. Given the good solubility of MPD and high volatility of acetone, it was used for rinsing the excess MPD from the valleys of patterned supports before IP. PAN supports were used due to their relatively higher chemical stability, hence TFC layers were obtained over PAN supports prepared using casting knife with pattern height of 900 µm. Obtained TFC membranes resulted in high permeance with a very low selectivity when applied in filtration for 2 g/L $MgSO_4$ solution at 15 bar (*Fig. 12*). This could be because of complete removal of MPD from the supports while rinsing with acetone leading to almost no or very little extent of IP. Other possibility could be due to the very high pattern height of the supports, thin film PA layer could not follow the crests and troughs of patterned support and there were many cracks which the allowed fluid and salt to pass through it. Therefore, this method of IP was eliminated at a very early stage of this study and casting knives with smaller patterns were used in the further membrane casting.

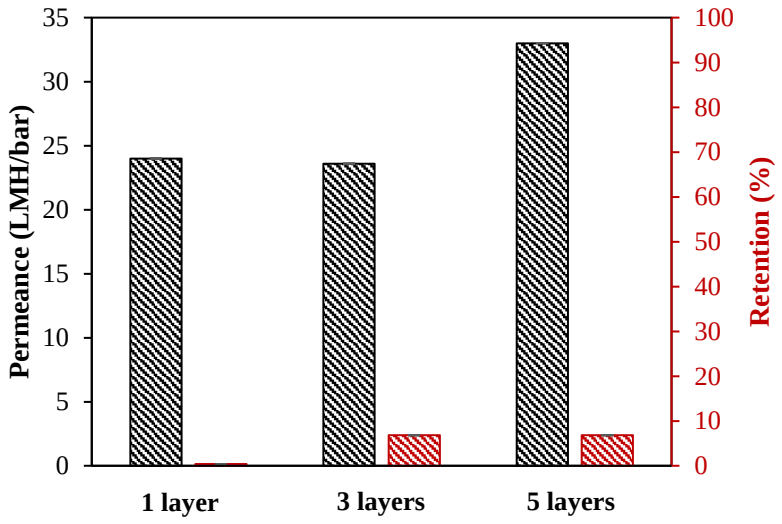

Fig. 12. *Permeance and retention given TFC membranes over PAN supports prepared through first technique of IP i.e. when excess MPD were removed by rinsing with acetone*

4.2. Effect of excess MPD removal by spin-assisted drying

Drying of excess MPD from the valleys of patterned supports was then assisted with a spin-coater. In order to further optimize the membrane performance, MPD concentration was varied from 0.5 - 2.5 wt% and 1-3 layers of PA were deposited to cover any defects due to pattern heights. This makes a total of 30 different TFC membranes with 2 different PSf supports (*Table A-1*) i.e. PSf_{500} and PSf_{700}. 3-layered TFC, h-PAN_{700} and X-linked PI_{700} were prepared to study the effect of different support materials. SEM cross-section images of PSf supports prepared using casting knife with pattern height of 500 and 700 µm resulted in support with the patterns

height of ca. 150 µm and 180 µm respectively (*Fig. 13 a, b*). PSf_{500} and PSf_{700} supports resulted in ca. 17 % and 20 % higher effective surface, respectively as compared to the flat counterparts.

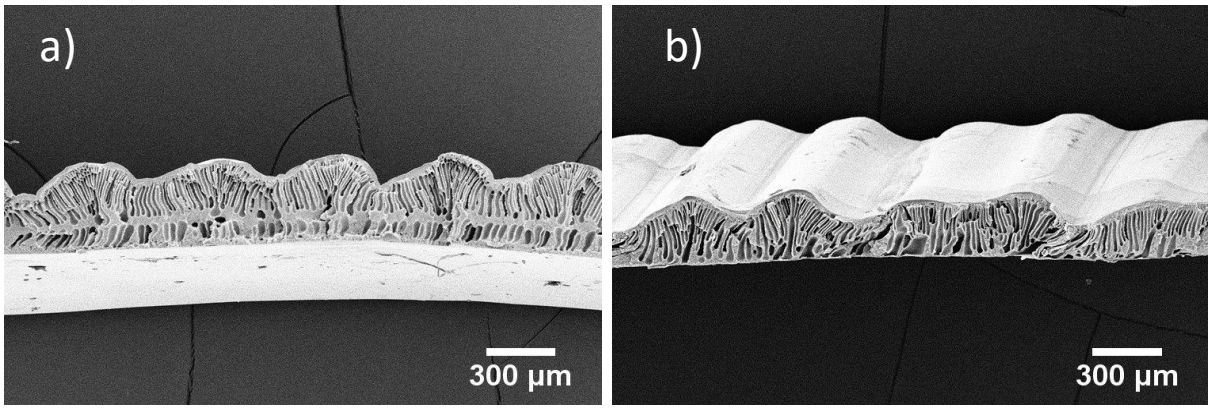

Fig. 13. *Cross-section SEM image of PSf support prepared using casting knife having (a) 500 µm and (b) 700 µm*

Next, the effects of different MPD concentrations, IP layers, pattern height and polymer supports on permeance and retention of the TFC membranes prepared using the spin assisted method are discussed.

4.2.1. Influence of varying MPD concentration

In order to study the influence of MPD concentration, concentrations of other additives (TEA, SDS) and monomer (TMC) were kept constant. For one layered PSf_{500} TFC membranes, increase in MPD concentration resulted in a decrease in membrane permeance along with a gradual increase in salt rejection. Membranes with 2.5 wt% MPD resulted in a maximum retention of 84.8 ± 2.0 % with ca. 1.9 LMH/bar (L m^{-2} h^{-1} bar^{-1}) permeance (*Fig. 14*). The trend of increasing salt rejection and decreasing permeance with gradual increment in MPD concentration is consistent with the study conducted for flat membranes [67]. In general, excess of MPD is crucial to allow sufficient transfer of MPD from the aqueous phase to organic phase. Higher MPD/TMC ratios are expected to provide higher cross-linking and an enhanced salt rejection. Further in-depth characterization can facilitate the finding of optimum MPD/TMC ratio for such membranes. However, additional IP layers were deposited in order to study their effect on the permeance and rejection of patterned TFC membranes. Low retention and high permeance in case of outlier membrane prepared using 2 wt % MPD (*Fig. 14*) could be due to the possible defect in the support membrane.

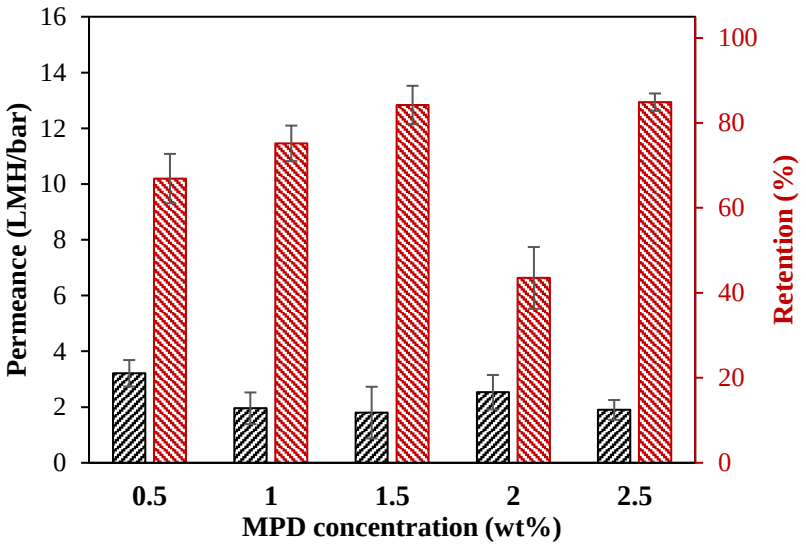

Fig. 14. *Effect of different MPD concentration on retention and permeance for one-layered PSf_{500} TFC membranes*

SEM surface images of TFC membranes (PSf_{500}), confirm the presence PA thin film layer (*Fig. 15*). Agglomeration or clustering of polymer network could be observed which reduces the salt retention of TFC membranes [68]. However, further AFM analysis of these membranes can elaborate their surface roughness at different MPD concentrations.

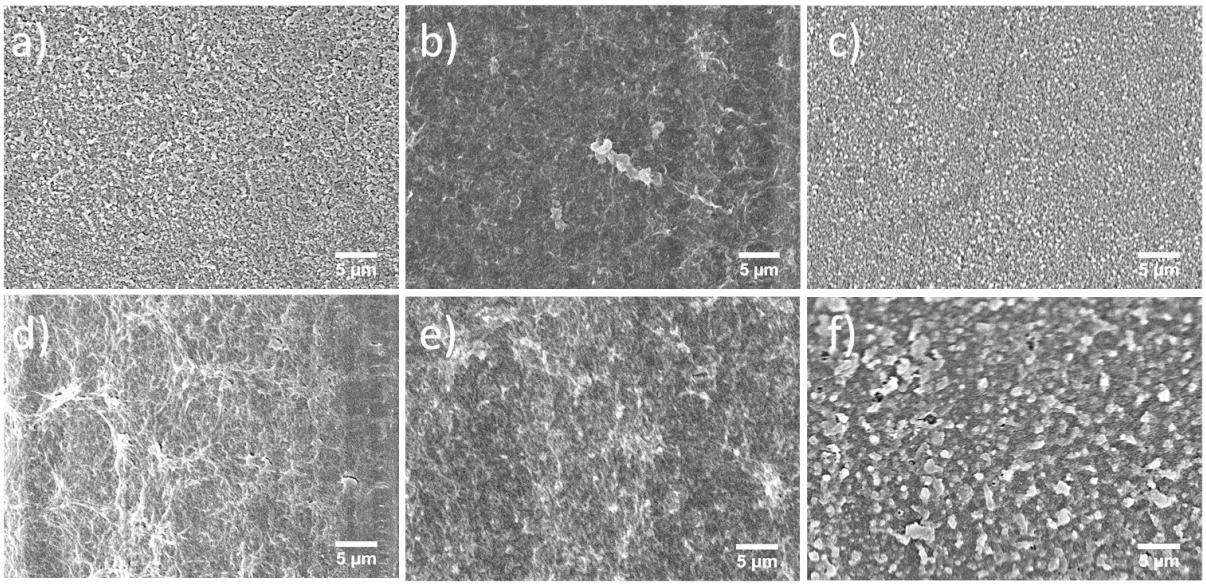

Fig. 15. *Surface images of (a) flat TFC membrane prepared on PSF/PEG support, (b) $PSf_{500}^{0.5\_1L}$, (c) $PSf_{500}^{1\_1L}$, (d) $PSf_{500}^{1.5\_1L}$, (e) $PSf_{500}^{2\_1L}$ and (f) $PSf_{500}^{2.5\_1L}$*

4.2.2. Influence of spin-coater assisted layer by layer thin film formation

Through spin assisted layer by layer thin film deposition 1, 2 and 3 PA layers were obtained separately on PSf supports having two pattern heights using five MPD solutions of different concentrations. Effect of layers and pattern heights on permeance and retention for TFC

membranes produced using each MPD solutions (0.5, 1, 1.5, 2 and 2.5 wt%) are discussed separately.

4.2.2.1. TFC membranes prepared using 0.5 wt% MPD

TFC membranes were prepared over PSf_{500} and PSf_{700} supports in order to simultaneously study the effect of pattern height and PA layers. $PSf_{500}^{0.5\_3L}$ resulted in retentions upto 95.1 ± 4.8 % at a permeance of 0.91 ± 0.078 LMH/bar when used for the filtration of 2 g/L $MgSO_4$ at 15 bar (*Fig. 16 a*). For PSf_{500}, permeance decreased from 3.31 ± 0.7 LMH/bar to 0.91 ± 0.78 LMH/bar and retention gradually increases from 66.6 ± 9.9 % to 95.1 ± 4.8 % with increment in PA layers (*Fig. 16 a*). This is due to the increased top layer thickness with increased number of IP cycles. Whereas, TFC membranes prepared over PSf_{700}^{3L} gives retention only up to 66.6 ± 9.9 %, which is way less than PSf_{500} membranes, while similar permeance of 0.8 LMH/bar was observed (*Fig. 16 b*). The lower retentions for PSf_{700} could be attributed to the lower extent of IP associated with low MPD concentrations, as higher surface area was exposed to IP compared to PSf_{500} supports. This could result in a thin PA top layer, which can be highly susceptible to cracking because of higher pattern heights (*Fig. A-8*).

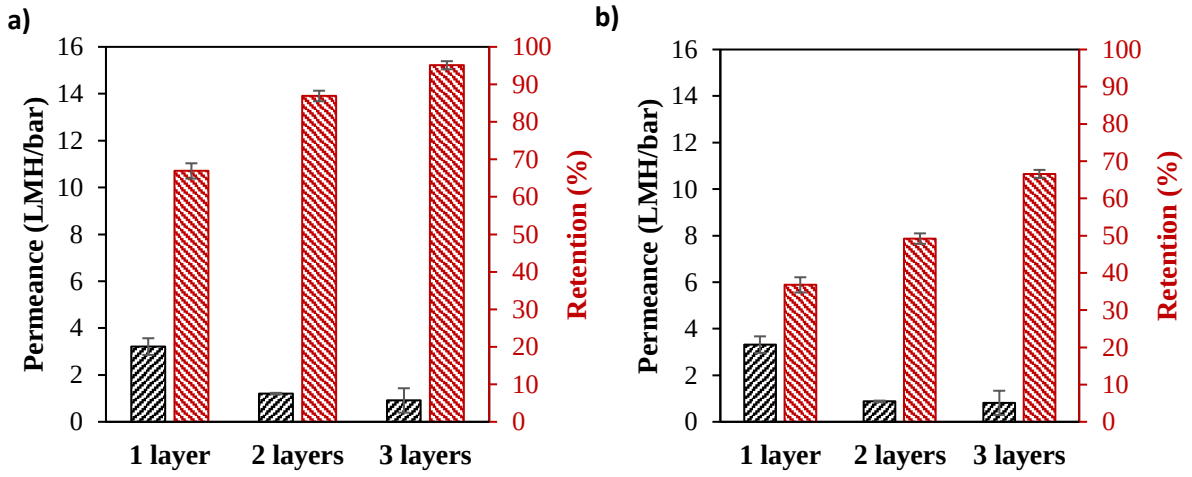

Fig. 16. *Permeance and retention given by TFC membranes prepared using 0.5 wt% MPD solution for 1, 2 and 3 layers of PA over (a) smaller patterned support and (b) larger patterned support*

4.2.2.2. TFC membranes prepared using 1 wt% MPD

$PSf_{500}^{1\_3L}$ membrane resulted in a maximum retention of 97.7 ± 5.8 % at a permeance of 0.91 LMH/bar (*Fig. 17 a*). The retention in this case is a little higher than that of $PSf_{500}^{0.5\_3L}$, which is expected since at increased MPD concentration, the extent of IP would also be higher. Surprisingly, $PSf_{500}^{1\_2L}$ membrane gives a very low retention and unexpectedly high permeance, this could be due to the defect in the support. PSf_{700} TFC membranes again showed lower retentions than PSf_{500} membranes, suggesting less selective PA layer formed due to

relatively wider pore size distribution and increase in the surface area exposed to IP reaction (*Fig. 17 b*).

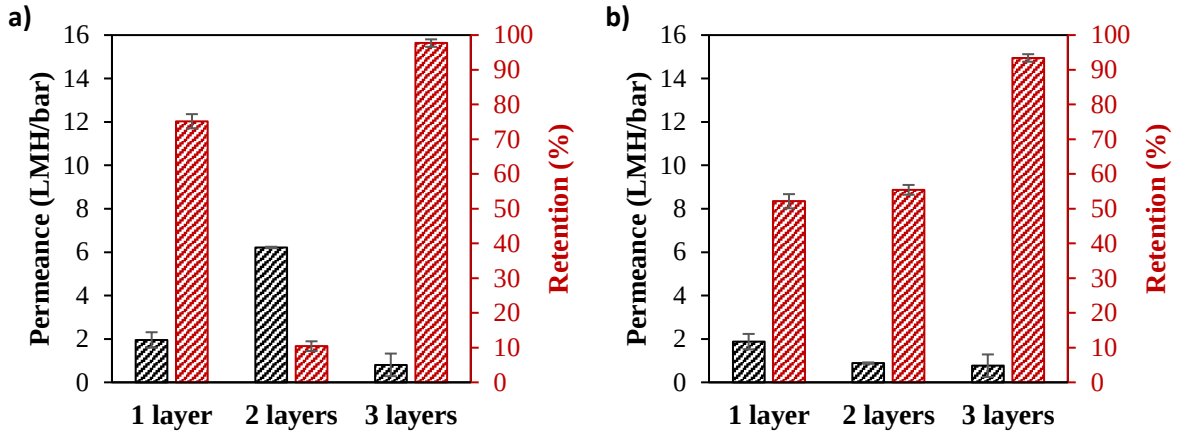

Fig. 17. *Permeance and retention given by TFC membranes prepared using 1 wt% MPD solution for 1, 2 and 3 layers of PA over (a) smaller patterned support and (b) larger patterned support*

4.2.2.3. TFC membranes prepared using 1.5 wt% MPD

$PSf_{500}^{1.5\_1L}$ resulted in retention of 84.2 ± 7.8 % at relatively higher permeance of 1.8 ± 0.9 LMH/bar, while maximum retention of ca. 97 % at around 0.81 LMH/bar permeance was observed for $PSf_{500}^{1.5\_3L}$ membrane (*Fig. 18 a*). This suggests better crosslinking of MPD and TMC at higher MPD concentrations. Similarly, $PSf_{700}^{1.5\_1L}$ also showed improved retentions around 84 % at a permeance of ca. 3.9 LMH/bar (*Fig. 18 b*). Lower retention with lower permeance for $PSf_{700}^{1.5\_3L}$ could be attributed to the presence of small crack in the PA layer or the support.

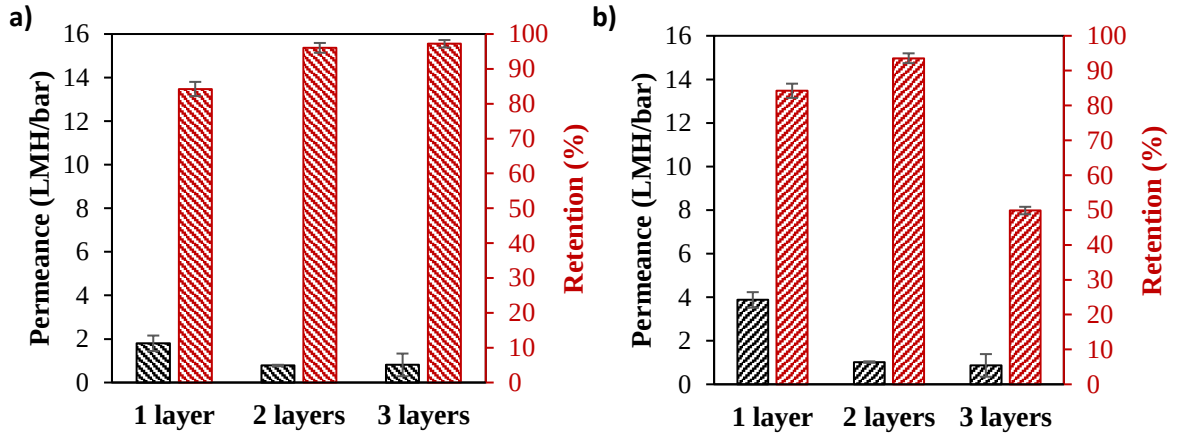

Fig. 18. *Permeance and retention given by TFC membranes prepared using 1.5 wt% MPD solution for 1, 2 and 3 layers of PA over (a) smaller patterned support and (b) larger patterned support*

4.2.2.4. TFC membranes prepared using 2 wt% MPD

Further increasing the MPD concentration resulted in higher retention of around 94 % at a permeance of ca. 1.7 LMH/bar for $PSf_{500}^{2\_2L}$. However, $PSf_{500}^{2\_1L}$ showed surprisingly lower

retention and relatively higher permeance (*Fig. 19 a*), which could be due to the presence of defects in the support itself. On the other hand, PSf_{700} based TFC membranes as usual resulted in lower retentions with lower permeance due to previously stated reasons (*Fig. 19 b*).

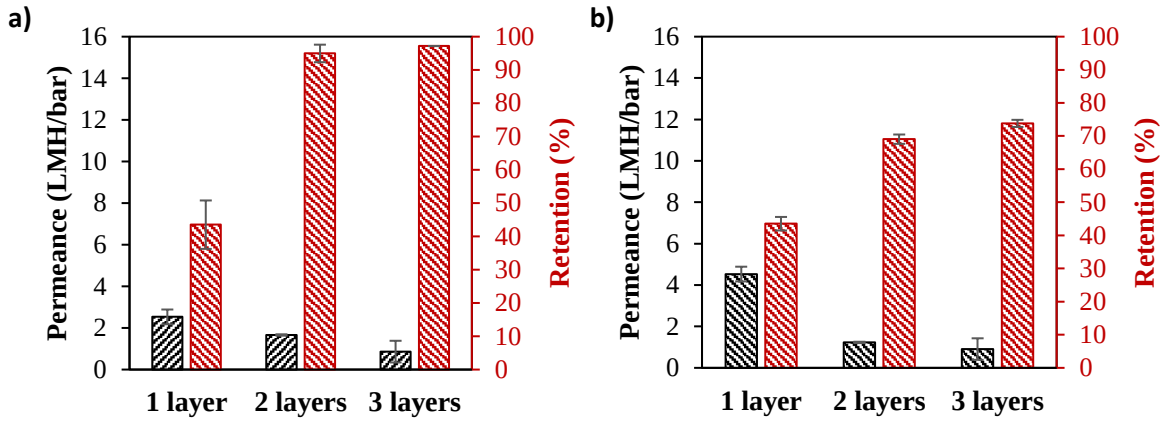

Fig. 19. *Permeance and retention given by TFC membranes prepared using 2 wt% MPD solution for 1, 2 and 3 layers of PA over (a) smaller patterned support and (b) larger patterned support*

4.2.2.5. TFC membranes prepared using 2.5 wt% MPD

$PSf_{500}^{2.5\_1L}$ showed a retention of around 85% with ca. 1.84 LMH/bar permeance (*Fig. 20 a*), which is comparable to the retention and permeance shown by $PSf_{500}^{1.5\_1L}$ and $PSf_{500}^{2\_1L}$ (*Fig. 18 a, 19 a*). Furthermore, no significant change in retention and permeance was observed for the TFC membranes prepared using higher MPD concentrations than 1.5 wt%. However, 2 layered IP for 2 wt% MPD and 0.1 wt% TMC concentration could be optimum for PSf_{500} supports with 94% $MgSO_4$ retention and a permeance of 1.66 LMH/bar. On the other hand, improved results were obtained for PSf_{700} supports at 2.5 wt% MPD concentration. $PSf_{700}^{2.5\_1L}$ showed around 84 % retentions and a permeance of ca. 1.86 LMH/bar, this suggests need for higher monomer concentrations for supports with higher patterned heights in order to have optimum MPD/TMC ratio for better cross-linking and presence of enough MPD diffused into the organic phase during reaction. At optimum MPD/TMC ratio, most acid chloride groups from TMC can react with MPD to be converted virtually to a PA film. However, possibly lack of sufficient TMC due to higher exposed surface area did not allow to form a uniform dense selective layer across the membrane surface for PSf_{700} supports. Hence, there is further need to investigate the effect of increased TMC concentration for PSf_{700} supports, it could not be included in this study due to time limitations.

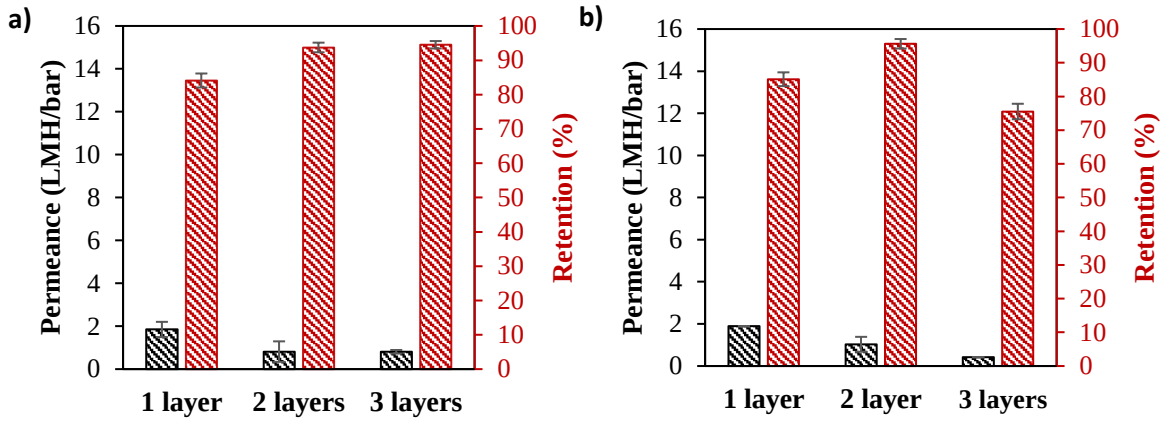

Fig. 20. *Permeance and retention given by TFC membranes prepared using 2.5 wt% MPD solution for 1, 2 and 3 layers of PA over (a) smaller patterned support and (b) larger patterned support*

Cross-section SEM images of TFC membranes (PSf_{500}) prepared using 2.5 wt% MPD concentration show that the thickness of thin film layer gradually increases with increase in IP layers (*Fig. 21*). Higher thickness of thin film selective layer could be attributed to higher selectivity and lower permeance in case of 3 layered membranes in all cases.

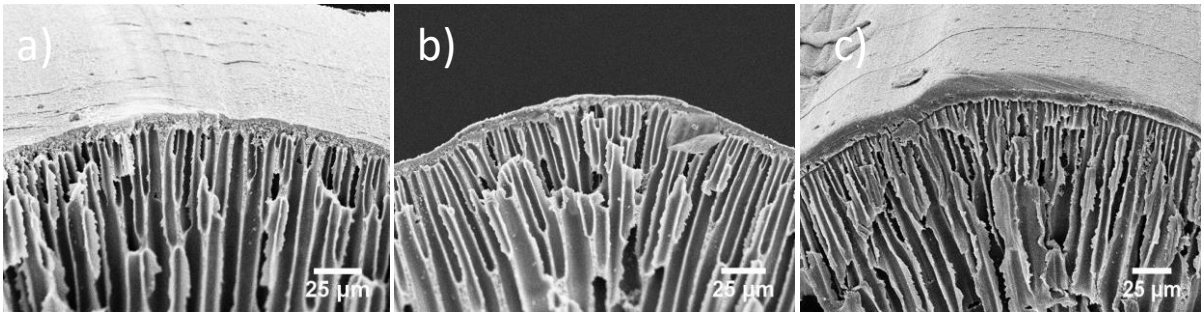

Fig. 21. *Cross section SEM images of (a) 1 layered, (b) 2 layered and (c) 3 layered TFC membranes prepared using 2.5 wt % MPD*

FTIR curve of 1, 2 and 3 layered TFC membranes ($PSf_{500}^{2.5\_1L}$, $PSf_{500}^{2.5\_2L}$, $PSf_{500}^{2.5\_3L}$) further confirms the synthesis of TFC PA layers over the support (*Fig. 22*).

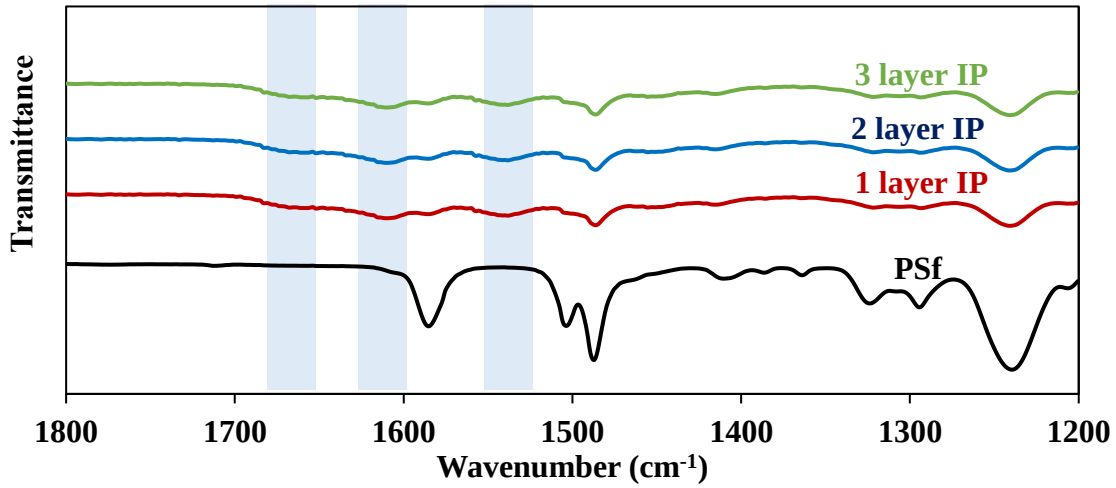

Fig. 22. *FTIR curve of 1,2 and 3 layered TFC membranes compared to that of PSf supports*

Characteristic peaks of aromatic PA could be seen at around 1670 cm^{-1}, 1609 cm^{-1} and 1540 cm^{-1} assigned to C=O stretching , aromatic ring breathing and C-N stretching, respectively [69]. Not much change in the FTIR curve of 1, 2 and 3 layered TFC membrane was observed. However, the characteristic peaks of PSf showed 70 % lower intensities for the TFC membrane as compared to the pristine PSf membranes, which suggests thicker PA layer.

4.4. Effect of different support materials

To study the influence of different patterned supports, PSf_{500} supports were compared to the X-PI_{500} and PAN_{500}. Concentrations of MPD and TMC were kept constant as 2.5 wt% and 0.1 wt%, respectively. 18wt% PSf with 20wt% PEG, 24wt% PI and 17wt% PAN supports were used. PAN and X-PI support membranes resulted in pattern heights of about ca. 30 µm and ca. 80 µm, respectively (*Fig. A-9*). It must be noted here that the upper limit pore size for an optimum support layer is approximately 100 nm. Smaller pore size reduces the overall mass transfer and the intrinsically lower permeance of the support significantly reduces the permeance of TFC membrane. On the other hand, in case of larger pore sizes, they can be plugged with the PA layer, resulting in thinner top layer, which is more prone to defect formation or porous structure, consequently resulting in lower salt rejection efficiency [68]. Adhesion between thin film layer and support also plays an important role in TFC membrane performance.

Fig. 23 shows the permeance and rejection for $PSf_{500}^{2.5\_3L}$, X-$PI_{500}^{2.5\_3L}$ and $PAN_{500}^{2.5\_3L}$ TFC membranes. Presence of characteristic PA peaks in FTIR and typical ridge and valley morphology on surface SEM images further confirms the top layer formation (*Fig. A-10, 11*) $PAN_{500}^{2.5\_3L}$ shows lowest retention of around 56 % with ca. 0.41 LMH/bar permeance. While X-$PI_{500}^{2.5\_3L}$ showed around 95 % but at a very low permeance of 0.023 LMH/bar. Whereas, $PSf_{500}^{2.5\_3L}$ resulted in around 95.5 % retention at relatively higher permeance of 0.81 LMH/bar.

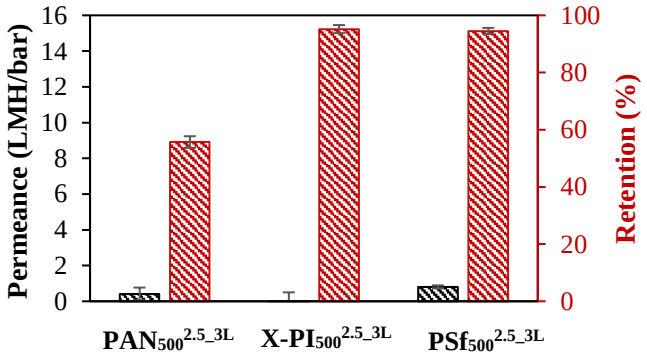

Fig. 23. *Permeance and retention comparison of TFC membranes prepared over different supports with same pattern height*

The significantly lower permeance for X-$PI_{500}^{2.5\_3L}$ can be attributed to the relatively lower pore size (Mean pore size: 60 nm) of the support, which additionally reduced the TFC permeance. On the other hand, lower retentions for $PAN_{500}^{2.5\_3L}$ might be due to the relatively wider pore size distribution, given in [43], which results in less selective PA top layer. However, it may be possible that one layered x-linked PI or PAN TFC membrane prepared at different conditions could give better results, further extensive optimization of various parameter is required in that case.

4.5. Effect of different MPD removal methods-Background work

PSf_{500} UF supports were used with monomers concentrations of 2.5 wt% MPD and 0.1 wt% TMC. Improper removal of excess MPD can lead to formation of weak PA layer formed over droplets, which is highly prone to breakage. Various methods were employed to remove the excess MPD including rubber wiper, lag time step of 10 min before IP, Kimwipes™ (Kimtech Science™), cyclo-hexane washing, air knife and spin-coater assisted drying (this work). As compared to the conventional flat-PSf membranes, patterned TFC membranes prepared via spin-coater assisted showed 150 % higher permeance, compensated with reduction in retention i.e. 85 % from 98 % (*Fig. 24*).

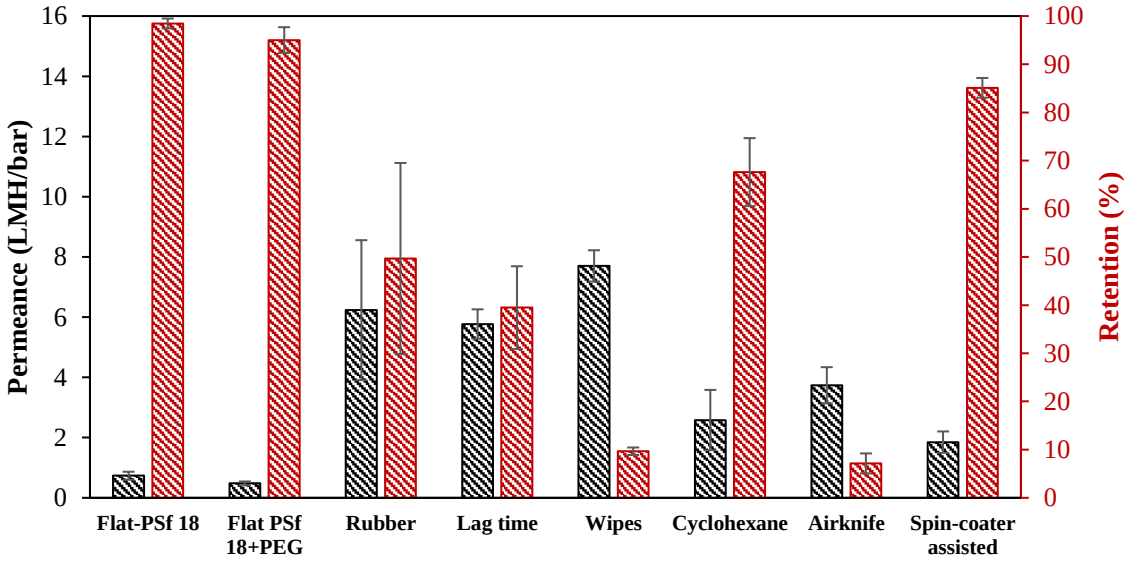

Fig. 24. *Comparison of retention and permeance value of TFC membrane prepared using different excess MPD removal method with the flat PSf and flat PSf/PEG membranes*

4.6. Effect of patterns on membrane fouling

Several studies have been conducted via mathematical modelling and experimental validation to examine the efficiency of membrane patterns for fouling mitigation [34,35,42]. CFD analysis of fluid flow over the membranes with pattern height same as the ones developed in this study (pattern height were used in the model as obtained from SEM images) shows that the vortices

are formed in the valley regions between patterns (*Fig. 25 a*). Developed vortices provide an opportunity for the particles in the valleys to come back to the bulk flow reducing their settling down leading to less membrane fouling. Whereas the fluid velocity at the surface of the crest of patterns (*Fig. 25 a*) is significantly higher as compared to the fluid velocity at the surface of the flat membranes (*Fig. A-12)*, very high velocity at the pattern surface further hinders the particle's settling down there as well. In addition, *Fig. 25 (b)* also shows higher shear stress at the apexes of the patterns. These suppositions completely agree with the study reported by *Won et al.* [27], where latex particles were used for the CFD simulation and experimental validation. The study revealed that in the case of fluid flow at higher Reynolds number (ca. 1600), vortex developed at a shorter distance from the bulk flow, suggesting that the probability of particles returning to bulk flow was higher. However, in all cases, patterned membrane due to increased hydrodynamics and higher surface area can lead to reduced particle deposition and higher flux through the membrane.

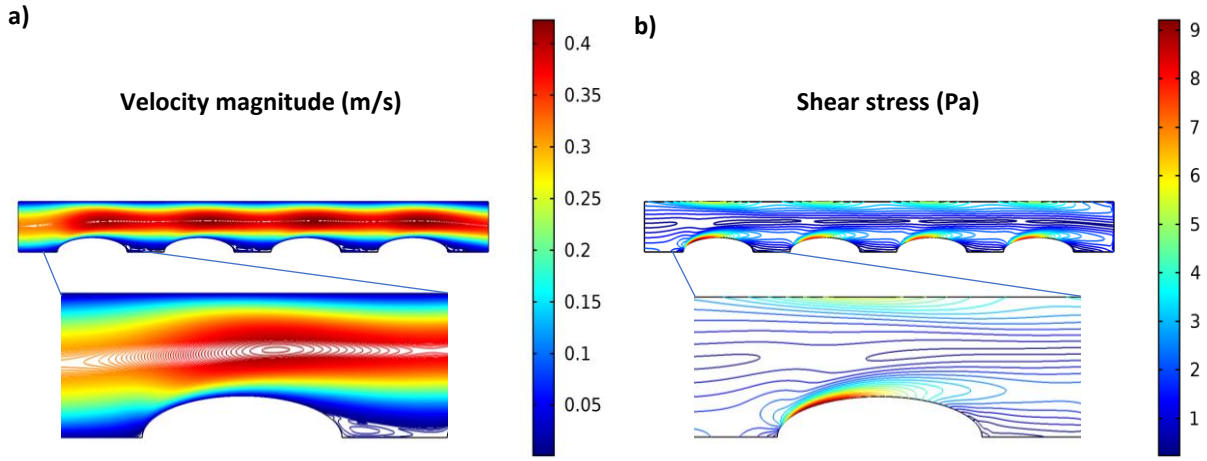

Fig. 25. *(a) Velocity profile and (b) shear stress profile of the fluid flow over the pattern membranes for the feed at an angle of 90 degrees to patterns*

5. Conclusions and Future Prospectives

5.1. Conclusions

Two ways of IP for TFC membrane preparation on three different kinds of micro-patterned support materials having different pattern heights was studied by varying various parameters. The following are the final conclusions of this study:

- The first IP technique in which excess MPD from the valleys was removed by rinsing with acetone resulted in membranes with significantly lower salt retention with high

water permeances. Hence, this technique was found inadequate for the TFC membranes preparation on patterned supports.

- The second IP method i.e. spin assisted IP showed significant improvement and a maximum of 84.8 ± 2.0 % retention at 1.9 LMH/bar permeance for $PSf_{500}^{2.5\_1L}$ membrane was observed.
- With increased number of IP cycles i.e. spin assisted layer by layer thin film deposition, permeance was decreased, while higher retentions were observed with increase in IP cycles for both PSf_{500} and PSf_{700} supports. However, no significant change in retention was observed for the TFC membranes prepared using higher MPD concentrations than 1.5 wt% even with increased number of IP cycles.
- In general, it was found that the PSf_{500} membranes gave better retention and permeance than PSf_{700} at all MPD concentration, which suggests inadequate extent of IP at the used TMC concentration for PSf_{700} due to relatively higher exposed surface area to IP.
- 2 layered IP with 2 wt% MPD and 0.1 wt% TMC concentration (i.e. $PSf_{500}^{2\_2L}$) was found to be optimum for PSf_{500} supports with 94% $MgSO_4$ retention a permeance of 1.66 LMH/bar.
- $PSf_{500}^{2.5\_3L}$ resulted in optimum permeance and retention as compared to $X\text{-}PI_{500}^{2.5\_3L}$, $PAN_{500}^{2.5\_3L}$.
- Patterned TFC membranes prepared via spin-coater assisted IP for optimum conditions showed 137 % higher permeance with a small compromise in retention (94% from 98%) as compared to conventional flat-PSf membranes.

5.2. Future prospectives

With above mentioned conclusions and fluid dynamics analysis it could be established that the micro-patterned TFC membranes are effective and promising tool for water treatment application as it gives better permeance with a little compromise in retention and provides good anti-fouling tendency. However, further investigation is still needed in order to further exploit the potential use of s-NIPS UF patterned membranes as a support for TFC membranes. The following are the future recommendations:

- Effect of varying TMC concentration should be investigated as we concluded ratio of MPD/TMC was not adequate for larger patterned membranes. Also, studies suggest that higher TMC concentration gives better salt retentions [67].
- More in-depth characterization could be used for better understanding of extent of PA cross-linking such as X-ray photoelectron spectroscopy (XPS) for elemental analysis,

atomic force microscopy (AFM) for pattern characterization and transmission electron microscopy (TEM) for the PA cross-sectional morphology analysis.

- X-linked PI UF supports can be a suitable candidate for further optimization in order to achieve better performing TFC membranes.
- Effect of spin assisted LBL PA deposition should be investigated for higher pattern heights to fully exploit the potential of s-NIPS micro-patterned supports.
- Effect of other PA formation chemistries should be studied as it has been reported previously that piperazine (PIP) in some cases tends to form a much smoother PA layer over patterned supports [70].

References

[1] R. Singh, Introduction to membrane technology, in: Hybrid Membrane Systems for Water Purification, Elsevier, 2005: pp. 1–56. https://doi.org/10.1016/B978-185617442-8/50002-6.

[2] A. Saxena, B.P. Tripathi, M. Kumar, V.K. Shahi, Membrane-based techniques for the separation and purification of proteins: An overview, Advances in Colloid and Interface Science. 145 (2009) 1–22. https://doi.org/10.1016/j.cis.2008.07.004.

[3] The United Nations world water development report 2020: water and climate change, in: 2020: pp. 1–9. https://unesdoc.unesco.org/ark:/48223/pf0000372985.locale=en.

[4] P.H. Gleick, Pacific Institute for Studies in Development, Environment, and Security, Stockholm Environment Institute, eds., Water in crisis: a guide to the world's fresh water resources, Oxford University Press, New York, 1993.

[5] T. Stephenson, ed., Membrane bioreactors for wastewater treatment, IWA Pub, London, UK, 2000.

[6] Y. Han, Z. Xu, C. Gao, Ultrathin Graphene Nanofiltration Membrane for Water Purification, Adv. Funct. Mater. 23 (2013) 3693–3700. https://doi.org/10.1002/adfm.201202601.

[7] A.M. Alklaibi, N. Lior, Membrane-distillation desalination: Status and potential, Desalination. 171 (2005) 111–131. https://doi.org/10.1016/j.desal.2004.03.024.

[8] M. Rickman, S. Maruf, E. Kujundzic, R.H. Davis, A. Greenberg, Y. Ding, J. Pellegrino, Fractionation and flux decline studies of surface-patterned nanofiltration membranes using NaCl-glycerol-BSA solutions, Journal of Membrane Science. 527 (2017) 102–110. https://doi.org/10.1016/j.memsci.2017.01.007.

[9] M.F.A. Goosen, S.S. Sablani, H. Al-Hinai, S. Al-Obeidani, R. Al-Belushi, D. Jackson, Fouling of Reverse Osmosis and Ultrafiltration Membranes: A Critical Review, Separation Science and Technology. 39 (2005) 2261–2297. https://doi.org/10.1081/SS-120039343.

[10] B. Van Der Bruggen, C. Vandecasteele, T. Van Gestel, W. Doyen, R. Leysen, A review of pressure-driven membrane processes in wastewater treatment and drinking water production, Environ. Prog. 22 (2003) 46–56. https://doi.org/10.1002/ep.670220116.

[11] J. Engler, Particle fouling of a rotating membrane disk, Water Research. 34 (2000) 557–565. https://doi.org/10.1016/S0043-1354(99)00148-7.

[12] T. Li, A.W.-K. Law, M. Cetin, A.G. Fane, Fouling control of submerged hollow fibre membranes by vibrations, Journal of Membrane Science. 427 (2013) 230–239. https://doi.org/10.1016/j.memsci.2012.09.031.

[13] P. v Zumbusch, W. Kulcke, G. Brunner, Use of alternating electrical fields as anti-fouling strategy in ultrafiltration of biological suspensions – Introduction of a new experimental procedure for crossflow filtration, Journal of Membrane Science. 142 (1998) 75–86. https://doi.org/10.1016/S0376-7388(97)00310-4.

[14] J.C.-T. Lin, D.-J. Lee, C. Huang, Membrane Fouling Mitigation: Membrane Cleaning, Separation Science and Technology. 45 (2010) 858–872. https://doi.org/10.1080/01496391003666940.

[15] N. Al-Bastaki, A. Abbas, Use of fluid instabilities to enhance membrane performance: a review, Desalination. 136 (2001) 255–262. https://doi.org/10.1016/S0011-9164(01)00188-6.

[16] Y.-J. Won, J. Lee, D.-C. Choi, H.R. Chae, I. Kim, C.-H. Lee, I.-C. Kim, Preparation and Application of Patterned Membranes for Wastewater Treatment, Environ. Sci. Technol. 46 (2012) 11021–11027. https://doi.org/10.1021/es3020309.

[17] I.M.A. ElSherbiny, A.S.G. Khalil, M. Ulbricht, Surface micro-patterning as a promising platform towards novel polyamide thin-film composite membranes of superior performance, Journal of Membrane Science. 529 (2017) 11–22. https://doi.org/10.1016/j.memsci.2017.01.046.
[18] Z. Yao, H. Guo, Z. Yang, W. Qing, C.Y. Tang, Preparation of nanocavity-contained thin film composite nanofiltration membranes with enhanced permeability and divalent to monovalent ion selectivity, Desalination. 445 (2018) 115–122. https://doi.org/10.1016/j.desal.2018.07.023.
[19] Q. Zhang, Z. Zhang, L. Dai, H. Wang, S. Li, S. Zhang, Novel insights into the interplay between support and active layer in the thin film composite polyamide membranes, Journal of Membrane Science. 537 (2017) 372–383. https://doi.org/10.1016/j.memsci.2017.05.033.
[20] L. Dong, X. Huang, Z. Wang, Z. Yang, X. Wang, C.Y. Tang, A thin-film nanocomposite nanofiltration membrane prepared on a support with in situ embedded zeolite nanoparticles, Separation and Purification Technology. 166 (2016) 230–239. https://doi.org/10.1016/j.seppur.2016.04.043.
[21] J. Mulder, Basic Principles of Membrane Technology, Springer Netherlands, 1996. https://books.google.de/books?id=tSlUcdPqnScC.
[22] H. Mariën, I.F.J. Vankelecom, Transformation of cross-linked polyimide UF membranes into highly permeable SRNF membranes via solvent annealing, Journal of Membrane Science. 541 (2017) 205–213. https://doi.org/10.1016/j.memsci.2017.06.080.
[23] R.D. Noble, S.A. Stern, eds., Membrane separations technology: principles and applications, Elsevier, Amsterdam ; New York, 1995.
[24] W.J. Koros, Y.H. Ma, T. Shimidzu, Terminology for membranes and membrane processes (IUPAC Recommendations 1996), Pure and Applied Chemistry. 68 (1996) 1479–1489. https://doi.org/10.1351/pac199668071479.
[25] R. Liang, A. Hu, M. Hatat-Fraile, N. Zhou, Fundamentals on Adsorption, Membrane Filtration, and Advanced Oxidation Processes for Water Treatment, in: A. Hu, A. Apblett (Eds.), Nanotechnology for Water Treatment and Purification, Springer International Publishing, Cham, 2014: pp. 1–45. https://doi.org/10.1007/978-3-319-06578-6_1.
[26] S. Badalov, Y. Oren, C.J. Arnusch, Ink-jet printing assisted fabrication of patterned thin film composite membranes, Journal of Membrane Science. 493 (2015) 508–514. https://doi.org/10.1016/j.memsci.2015.06.051.
[27] Y.-J. Won, S.-Y. Jung, J.-H. Jang, J.-W. Lee, H.-R. Chae, D.-C. Choi, K. Hyun Ahn, C.-H. Lee, P.-K. Park, Correlation of membrane fouling with topography of patterned membranes for water treatment, Journal of Membrane Science. 498 (2016) 14–19. https://doi.org/10.1016/j.memsci.2015.09.058.
[28] Y.-J. Won, D.-C. Choi, J.H. Jang, J.-W. Lee, H.R. Chae, I. Kim, K.H. Ahn, C.-H. Lee, I.-C. Kim, Factors affecting pattern fidelity and performance of a patterned membrane, Journal of Membrane Science. 462 (2014) 1–8. https://doi.org/10.1016/j.memsci.2014.03.012.
[29] A. Sotto, A. Rashed, R.-X. Zhang, A. Martínez, L. Braken, P. Luis, B. Van der Bruggen, Improved membrane structures for seawater desalination by studying the influence of sublayers, Desalination. 287 (2012) 317–325. https://doi.org/10.1016/j.desal.2011.09.024.
[30] S.H. Maruf, A.R. Greenberg, J. Pellegrino, Y. Ding, Critical flux of surface-patterned ultrafiltration membranes during cross-flow filtration of colloidal particles, Journal of Membrane Science. 471 (2014) 65–71. https://doi.org/10.1016/j.memsci.2014.07.071.
[31] P.Z. Çulfaz, M. Wessling, R.G.H. Lammertink, Hollow fiber ultrafiltration membranes with microstructured inner skin, Journal of Membrane Science. 369 (2011) 221–227. https://doi.org/10.1016/j.memsci.2010.11.063.

[32] P.Z. Çulfaz, E. Rolevink, C. van Rijn, R.G.H. Lammertink, M. Wessling, Microstructured hollow fibers for ultrafiltration, Journal of Membrane Science. 347 (2010) 32–41. https://doi.org/10.1016/j.memsci.2009.10.003.
[33] K. Scott, J. Lobato, Mass transfer characteristics of cross-corrugated membranes, Desalination. 146 (2002) 255–258. https://doi.org/10.1016/S0011-9164(02)00483-6.
[34] S.Y. Jung, Y.-J. Won, J.H. Jang, J.H. Yoo, K.H. Ahn, C.-H. Lee, Particle deposition on the patterned membrane surface: Simulation and experiments, Desalination. 370 (2015) 17–24. https://doi.org/10.1016/j.desal.2015.05.014.
[35] J.H. Jang, J. Lee, S.-Y. Jung, D.-C. Choi, Y.-J. Won, K.H. Ahn, P.-K. Park, C.-H. Lee, Correlation between particle deposition and the size ratio of particles to patterns in nano- and micro-patterned membrane filtration systems, Separation and Purification Technology. 156 (2015) 608–616. https://doi.org/10.1016/j.seppur.2015.10.056.
[36] M.J. van der Waal, I.G. Racz, Mass transfer in corrugated-plate membrane modules. I. Hyperfiltration experiments, Journal of Membrane Science. 40 (1989) 243–260. https://doi.org/10.1016/0376-7388(89)89008-8.
[37] M. Ulbricht, Advanced functional polymer membranes, Polymer. 47 (2006) 2217–2262. https://doi.org/10.1016/j.polymer.2006.01.084.
[38] L. Vogelaar, J.N. Barsema, C.J.M. van Rijn, W. Nijdam, M. Wessling, Phase Separation Micromolding—PSμM, Adv. Mater. 15 (2003) 1385–1389. https://doi.org/10.1002/adma.200304949.
[39] S.H. Maruf, L. Wang, A.R. Greenberg, J. Pellegrino, Y. Ding, Use of nanoimprinted surface patterns to mitigate colloidal deposition on ultrafiltration membranes, Journal of Membrane Science. 428 (2013) 598–607. https://doi.org/10.1016/j.memsci.2012.10.059.
[40] O. Heinz, M. Aghajani, A.R. Greenberg, Y. Ding, Surface-patterning of polymeric membranes: fabrication and performance, Current Opinion in Chemical Engineering. 20 (2018) 1–12. https://doi.org/10.1016/j.coche.2018.01.008.
[41] M. Bikel, I.G.M. Pünt, R.G.H. Lammertink, M. Wessling, Micropatterned Polymer Films by Vapor-Induced Phase Separation Using Permeable Molds, ACS Appl. Mater. Interfaces. 1 (2009) 2856–2861. https://doi.org/10.1021/am900594p.
[42] N.U. Barambu, M.R. Bilad, Y. Wibisono, J. Jaafar, T.M.I. Mahlia, A.L. Khan, Membrane Surface Patterning as a Fouling Mitigation Strategy in Liquid Filtration: A Review, Polymers. 11 (2019) 1687. https://doi.org/10.3390/polym11101687.
[43] L. Marbelia, A. Ilyas, M. Dierick, J. Qian, C. Achille, R. Ameloot, I.F.J. Vankelecom, Preparation of patterned flat-sheet membranes using a modified phase inversion process and advanced casting knife construction techniques, Journal of Membrane Science. 597 (2020) 117621. https://doi.org/10.1016/j.memsci.2019.117621.
[44] W.J. Lau, A.F. Ismail, N. Misdan, M.A. Kassim, A recent progress in thin film composite membrane: A review, Desalination. 287 (2012) 190–199. https://doi.org/10.1016/j.desal.2011.04.004.
[45] R. Zhang, S. Yu, W. Shi, W. Wang, X. Wang, Z. Zhang, L. Li, B. Zhang, X. Bao, A novel polyesteramide thin film composite nanofiltration membrane prepared by interfacial polymerization of serinol and trimesoyl chloride (TMC) catalyzed by 4-dimethylaminopyridine (DMAP), Journal of Membrane Science. 542 (2017) 68–80. https://doi.org/10.1016/j.memsci.2017.07.054.
[46] G.R. Guillen, Y. Pan, M. Li, E.M.V. Hoek, Preparation and Characterization of Membranes Formed by Nonsolvent Induced Phase Separation: A Review, Ind. Eng. Chem. Res. 50 (2011) 3798–3817. https://doi.org/10.1021/ie101928r.
[47] J.E. Cadotte, Interfacially synthesized reverse osmosis membrane, Google Patents, 1981.
[48] B.J. Feinberg, E.M.V. Hoek, INTERFACIAL POLYMERIZATION, (n.d.) 15.
[49] I.M.A. ElSherbiny, R. Ghannam, A.S.G. Khalil, M. Ulbricht, Isotropic macroporous polyethersulfone membranes as competitive supports for high performance polyamide

desalination membranes, Journal of Membrane Science. 493 (2015) 782–793. https://doi.org/10.1016/j.memsci.2015.05.064.
[50] Z. Yao, H. Guo, Z. Yang, C. Lin, B. Zhu, Y. Dong, C.Y. Tang, Reactable substrate participating interfacial polymerization for thin film composite membranes with enhanced salt rejection performance, Desalination. 436 (2018) 1–7. https://doi.org/10.1016/j.desal.2018.01.039.
[51] J.-E. Gu, S. Lee, C.M. Stafford, J.S. Lee, W. Choi, B.-Y. Kim, K.-Y. Baek, E.P. Chan, J.Y. Chung, J. Bang, J.-H. Lee, Molecular Layer-by-Layer Assembled Thin-Film Composite Membranes for Water Desalination, Adv. Mater. 25 (2013) 4778–4782. https://doi.org/10.1002/adma.201302030.
[52] S.-H. Chen, D.-J. Chang, R.-M. Liou, C.-S. Hsu, S.-S. Lin, Preparation and separation properties of polyamide nanofiltration membrane, J. Appl. Polym. Sci. 83 (2002) 1112–1118. https://doi.org/10.1002/app.2282.
[53] R.J. Petersen, Composite reverse osmosis and nanofiltration membranes, Journal of Membrane Science. 83 (1993) 81–150.
[54] G.-Y. Chai, W.B. Krantz, Formation and characterization of polyamide membranes via interfacial polymerization, Journal of Membrane Science. 93 (1994) 175–192. https://doi.org/10.1016/0376-7388(94)80006-5.
[55] A.K. Ghosh, B.-H. Jeong, X. Huang, E.M.V. Hoek, Impacts of reaction and curing conditions on polyamide composite reverse osmosis membrane properties, Journal of Membrane Science. 311 (2008) 34–45. https://doi.org/10.1016/j.memsci.2007.11.038.
[56] X. He, T. Wang, Y. Li, J. Chen, J. Li, Fabrication and characterization of micro-patterned PDMS composite membranes for enhanced ethanol recovery, Journal of Membrane Science. 563 (2018) 447–459. https://doi.org/10.1016/j.memsci.2018.06.015.
[57] J.A. Kharraz, A.K. An, Patterned superhydrophobic polyvinylidene fluoride (PVDF) membranes for membrane distillation: Enhanced flux with improved fouling and wetting resistance, Journal of Membrane Science. 595 (2020) 117596. https://doi.org/10.1016/j.memsci.2019.117596.
[58] S.H. Maruf, A.R. Greenberg, Y. Ding, Influence of substrate processing and interfacial polymerization conditions on the surface topography and permselective properties of surface-patterned thin-film composite membranes, Journal of Membrane Science. 512 (2016) 50–60. https://doi.org/10.1016/j.memsci.2016.04.003.
[59] A.K. Ghosh, E.M.V. Hoek, Impacts of support membrane structure and chemistry on polyamide–polysulfone interfacial composite membranes, Journal of Membrane Science. 336 (2009) 140–148. https://doi.org/10.1016/j.memsci.2009.03.024.
[60] AutoJet Model 2008+ Spray Controller | Spraying Systems Co., (n.d.). https://www.spray.com/Products/Spray-Control-Options/AutoJet-Model-2008-Spray-Controller (accessed June 26, 2020).
[61] M. Dierick, Novel synthesis of patterned plyacrylonitrile membranes, Katholieke Universiteit Leuven, 2017.
[62] S. Yang, H. Zhen, B. Su, Polyimide thin film composite (TFC) membranes via interfacial polymerization on hydrolyzed polyacrylonitrile support for solvent resistant nanofiltration, RSC Adv. 7 (2017) 42800–42810. https://doi.org/10.1039/C7RA08133B.
[63] R. Thür, M. Corvilain, C. Klaysom, Y. Hartanto, I.F.J. Vankelecom, Tuning the selectivity of thin film composite forward osmosis membranes: Effect of co-solvent and different interfacial polymerization synthesis routes, Separation and Purification Technology. 227 (2019) 115671. https://doi.org/10.1016/j.seppur.2019.06.009.
[64] N.Y. Yip, A. Tiraferri, W.A. Phillip, J.D. Schiffman, M. Elimelech, High Performance Thin-Film Composite Forward Osmosis Membrane, Environ. Sci. Technol. 44 (2010) 3812–3818. https://doi.org/10.1021/es1002555.

[65] P. De Wint, Optimization of patterned polysulfone supports for thin film composite membranes, Katholieke Universiteit Leuven, 2019.
[66] A. Ilyas, Ongoing PhD research, Katholieke Universiteit Leuven, 2020. https://www.biw.kuleuven.be/m2s/cmacs/research/membrane-technology.
[67] B. Khorshidi, T. Thundat, B.A. Fleck, M. Sadrzadeh, Thin film composite polyamide membranes: parametric study on the influence of synthesis conditions, RSC Adv. 5 (2015) 54985–54997. https://doi.org/10.1039/C5RA08317F.
[68] P.S. Singh, S.V. Joshi, J.J. Trivedi, C.V. Devmurari, A.P. Rao, P.K. Ghosh, Probing the structural variations of thin film composite RO membranes obtained by coating polyamide over polysulfone membranes of different pore dimensions, Journal of Membrane Science. 278 (2006) 19–25. https://doi.org/10.1016/j.memsci.2005.10.039.
[69] S. Hermans, R. Bernstein, A. Volodin, I.F.J. Vankelecom, Study of synthesis parameters and active layer morphology of interfacially polymerized polyamide–polysulfone membranes, Reactive and Functional Polymers. 86 (2015) 199–208. https://doi.org/10.1016/j.reactfunctpolym.2014.09.013.
[70] S.H. Maruf, Z. Li, J.A. Yoshimura, J. Xiao, A.R. Greenberg, Y. Ding, Influence of nanoimprint lithography on membrane structure and performance, Polymer. 69 (2015) 129–137. https://doi.org/10.1016/j.polymer.2015.05.049.

Appendices

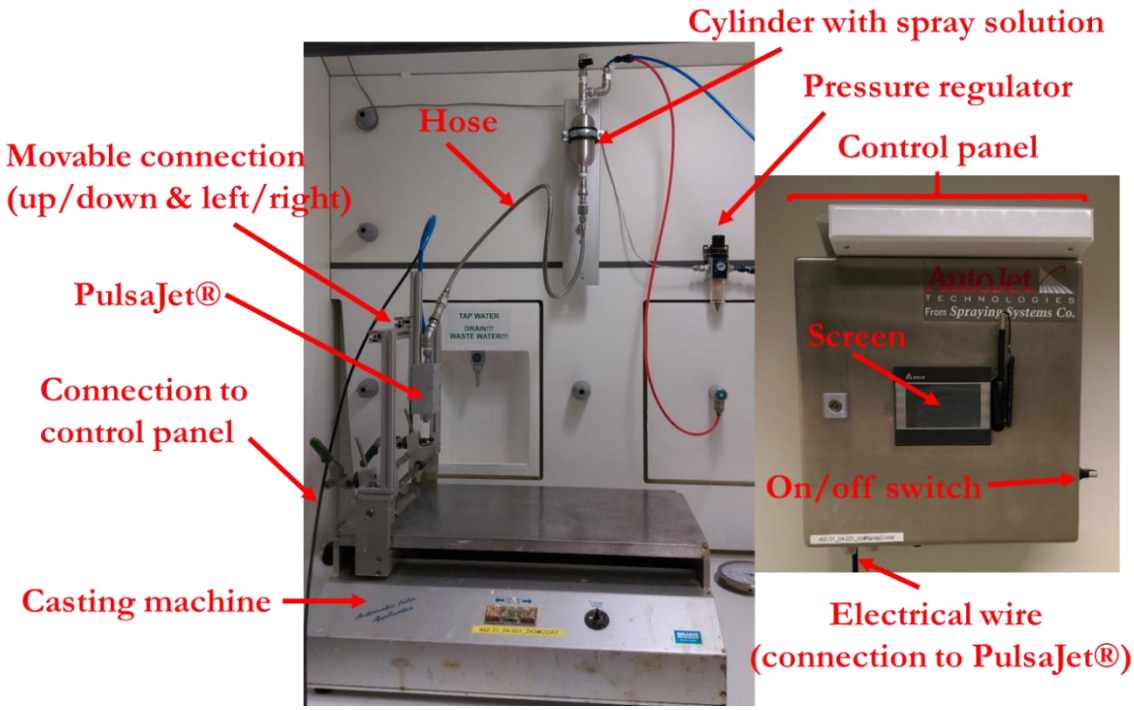

Figure A-1. *Detailed overview of AutoJet® Model 2008+ Spray Control Panel and its configuration for pattered membrane synthesis through s-NIPS*

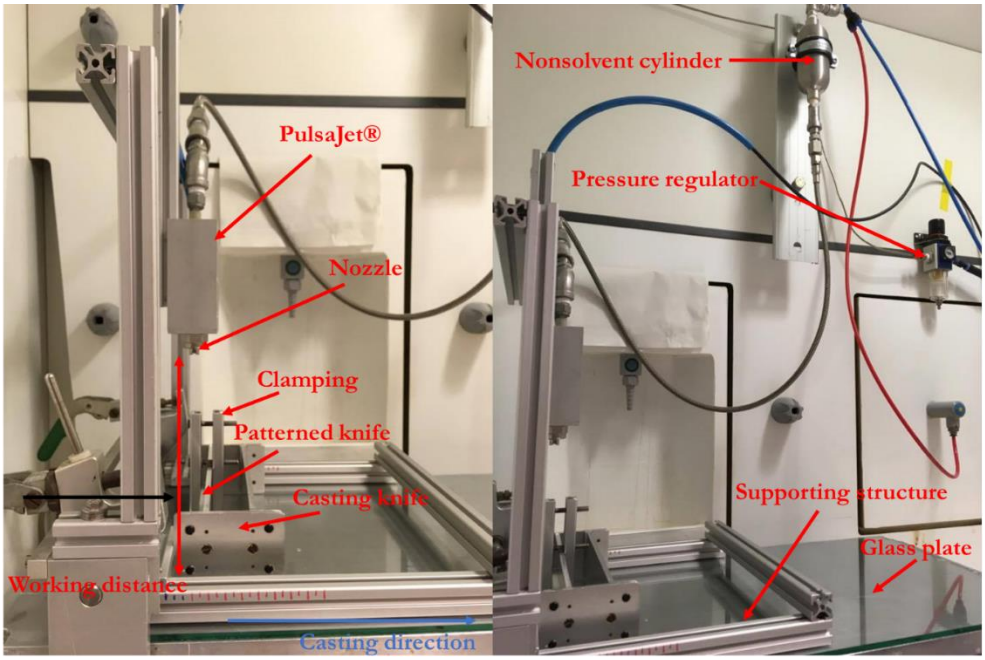

Figure A-2. *Detailed membrane casting set-up through s-NIPS, in this study patterned casting knife was not clamped but screwed to the conventional aluminum knife, adapted from [61]*

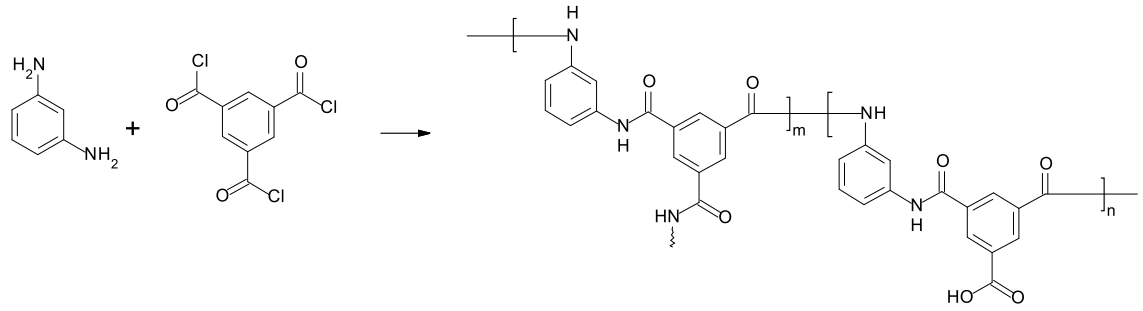

Figure A-3. *Reaction mechanism of interfacial polymerization: chemical structures of MPD, TMC and the product of IP; the carboxyl group in the product represents a hydrolysed acyl group*

Figure A-4. *In house developed interfacial polymerization set-up*

***Table A-1**. Complete table of TFC membranes prepared with PAN, PSf and x-linked PI supports with pattern height of 500 and 700 μ using 2nd technique of IP*

UF support	Membrane name*	MPD concentration (wt %)	Number of PA layers
PAN (900 μm)	PAN_{900}^{1L}	2.5	1
	PAN_{900}^{3L}	2.5	3
	PAN_{900}^{5L}	2.5	5
PSf (500 μm)	$PSf_{500}^{0.5\_1L}$	0.5	1
	$PSf_{500}^{0.5\_2L}$	0.5	2
	$PSf_{500}^{0.5\_3L}$	0.5	3
	$PSf_{500}^{1\_1L}$	1	1
	$PSf_{500}^{1\_2L}$	1	2
	$PSf_{500}^{1\_3L}$	1	3
	$PSf_{500}^{1.5\_1L}$	1.5	1
	$PSf_{500}^{1.5\_2L}$	1.5	2
	$PSf_{500}^{1.5\_3L}$	1.5	3
	$PSf_{500}^{2\_1L}$	2	1
	$PSf_{500}^{2\_2L}$	2	2
	$PSf_{500}^{2\_3L}$	2	3
	$PSf_{500}^{2.5\_1L}$	2.5	1
	$PSf_{500}^{2.5\_2L}$	2.5	2
	$PSf_{500}^{2.5\_3L}$	2.5	3
PSf (700 μm)	$PSf_{700}^{0.5\_1L}$	0.5	1
	$PSf_{700}^{0.5\_2L}$	0.5	2
	$PSf_{700}^{0.5\_3L}$	0.5	3
	$PSf_{700}^{1\_1L}$	1	1
	$PSf_{700}^{1\_2L}$	1	2
	$PSf_{700}^{1\_3L}$	1	3
	$PSf_{700}^{1.5\_1L}$	1.5	1
	$PSf_{700}^{1.5\_2L}$	1.5	2
	$PSf_{700}^{1.5\_3L}$	1.5	3

	$PSf_{700}^{2\_1L}$	2	1
	$PSf_{700}^{2\_2L}$	2	2
	$PSf_{700}^{2\_3L}$	2	3
	$PSf_{700}^{2.5\_1L}$	2.5	1
	$PSf_{700}^{2.5\_2L}$	2.5	2
	$PSf_{700}^{2.5\_3L}$	2.5	3
PAN (500 µm)	$h-PAN_{500}^{2.5\_3L}$	2.5	3
X-PI (500 µm)	$X-PI_{500}^{2.5\_3L}$	2.5	3

**The digit before L in the superscript represents number of PA layers, while the first part of the superscript represents concentration of MPD used. 900, 700 and 500 in subscript represents the pattern height of casting knife used.*

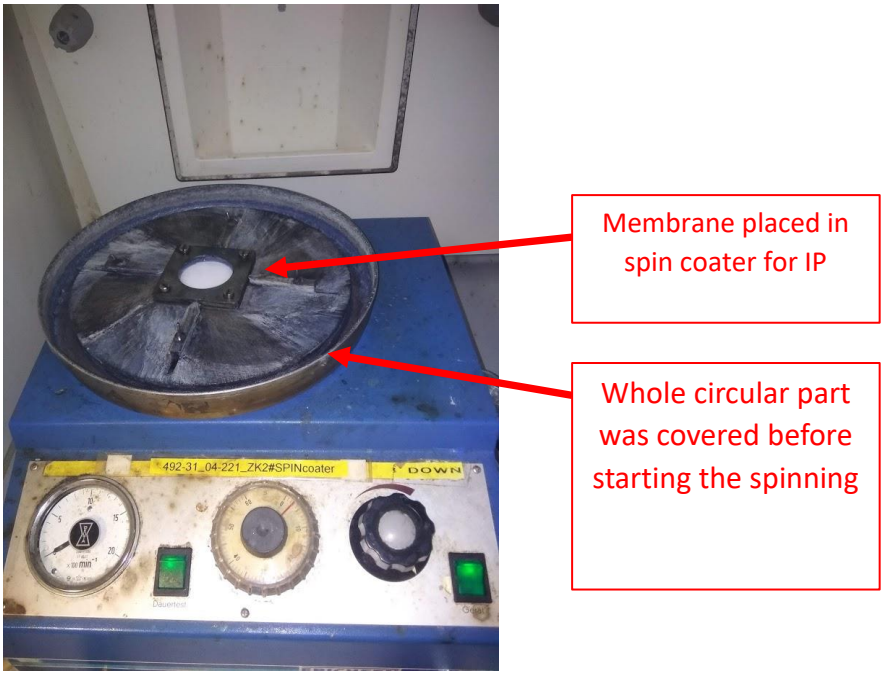

Figure A-5. *Spin coater system used for modified IP process*

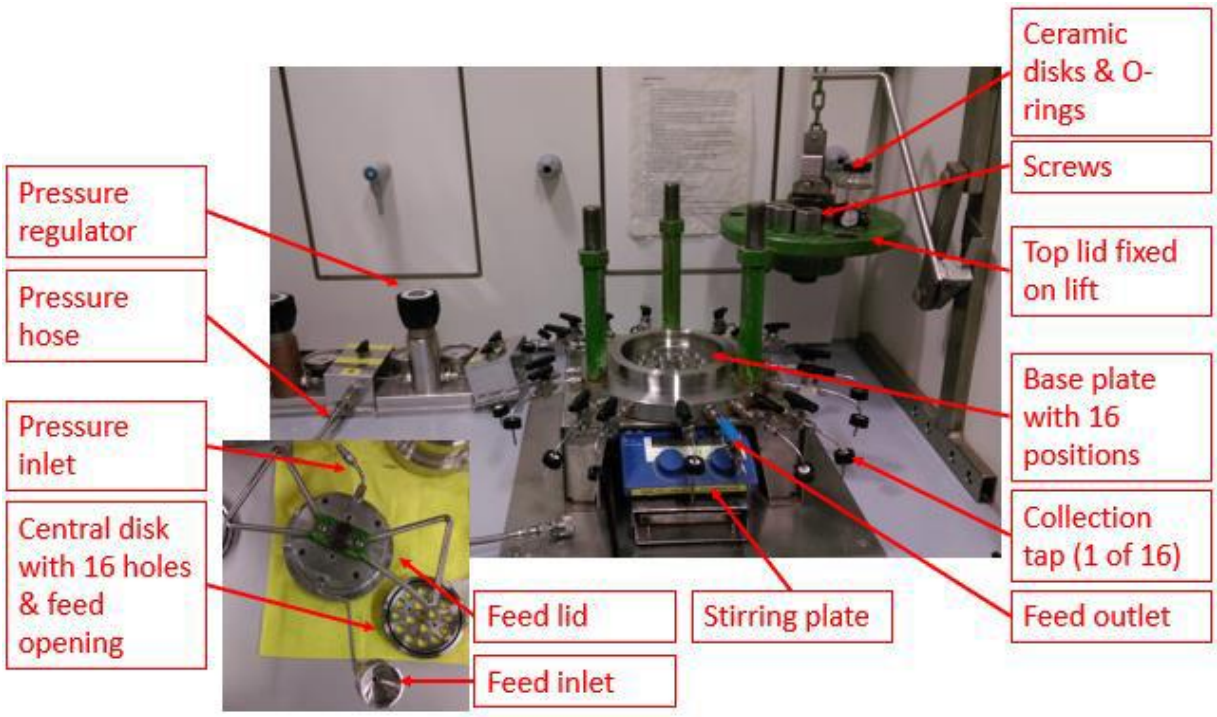

Figure A-6. *Overview of the Pressure-driven dead-end filtration set-up used in this study*

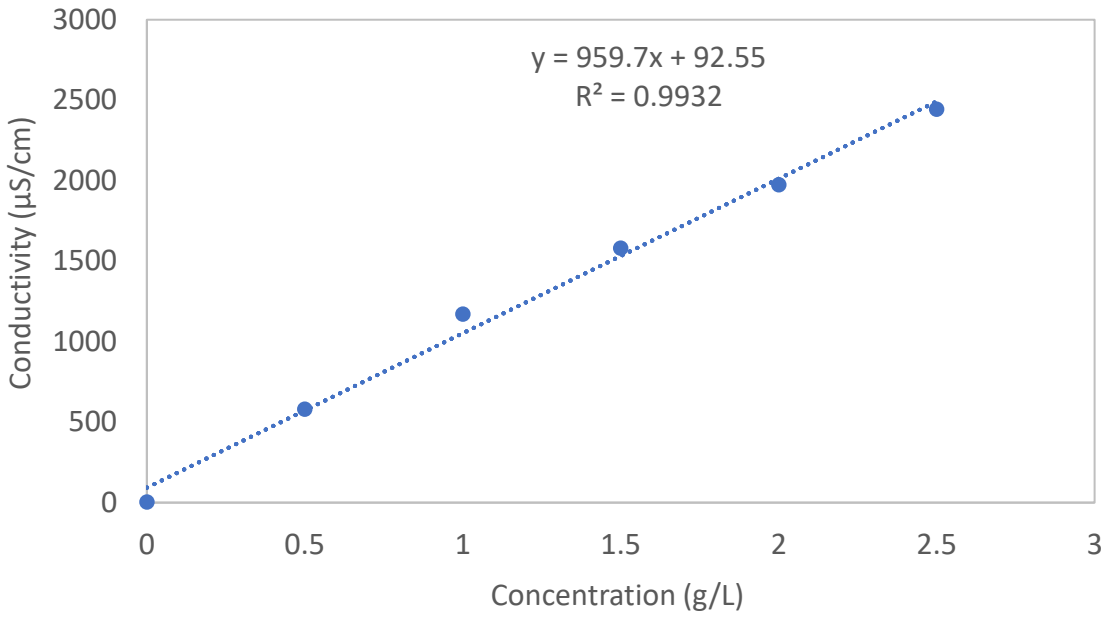

Figure A-7. *$MgSO_4$ concentration calibration curve*

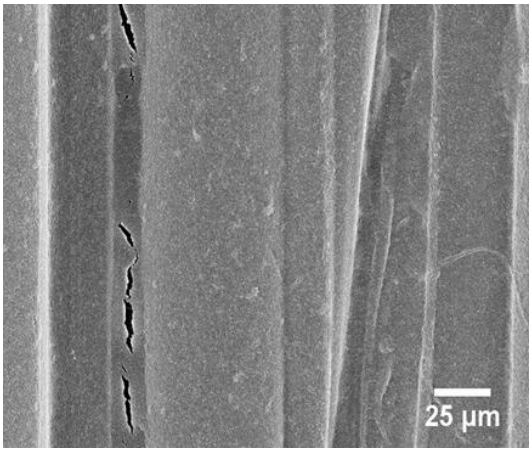

Figure A-8. *SEM surface image showing cracks in some cases*

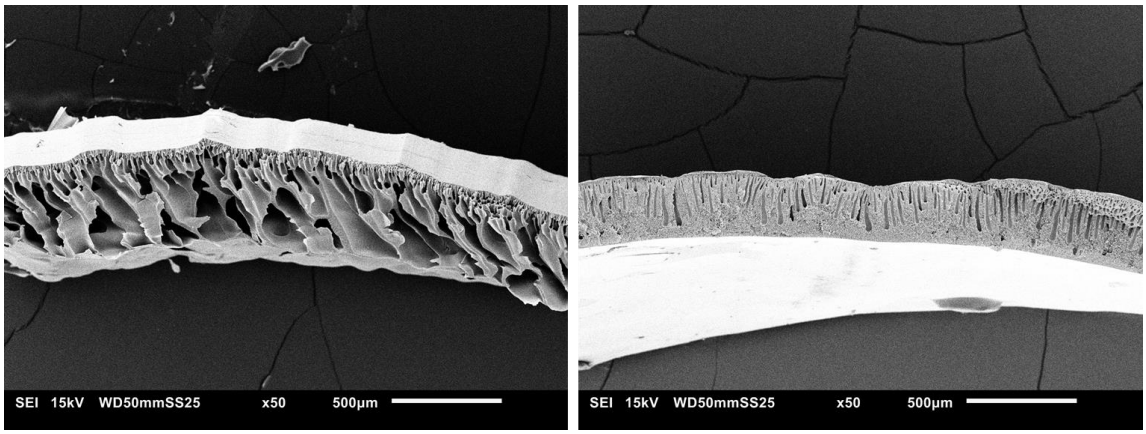

Figure A-9. *SEM cross-section of image of (a) PAN support and (b) PI support*

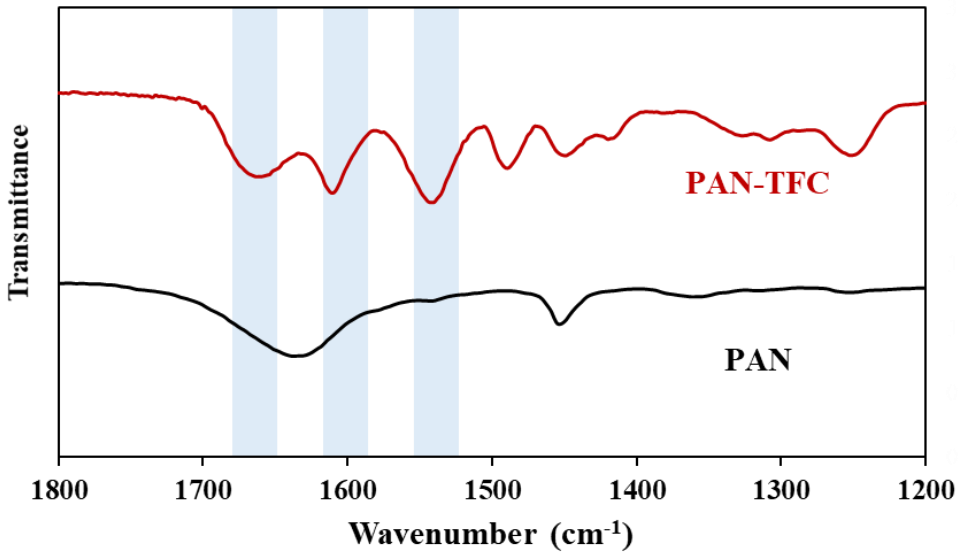

Figure A-10. *FTIR curve of PAN support and TFC membrane over PAN support*

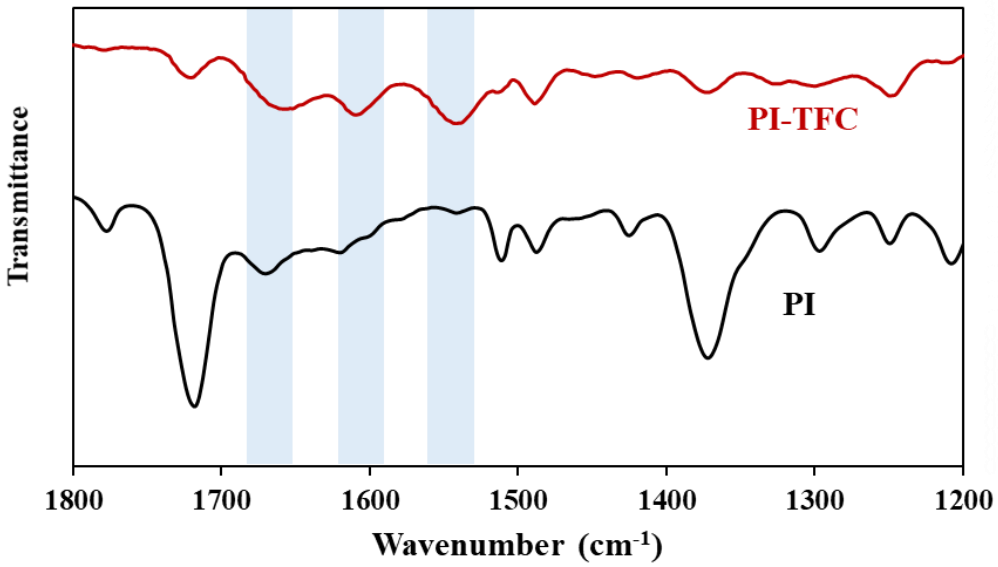

Figure A-11. *FTIR curve of PI support and TFC membrane over PI support*

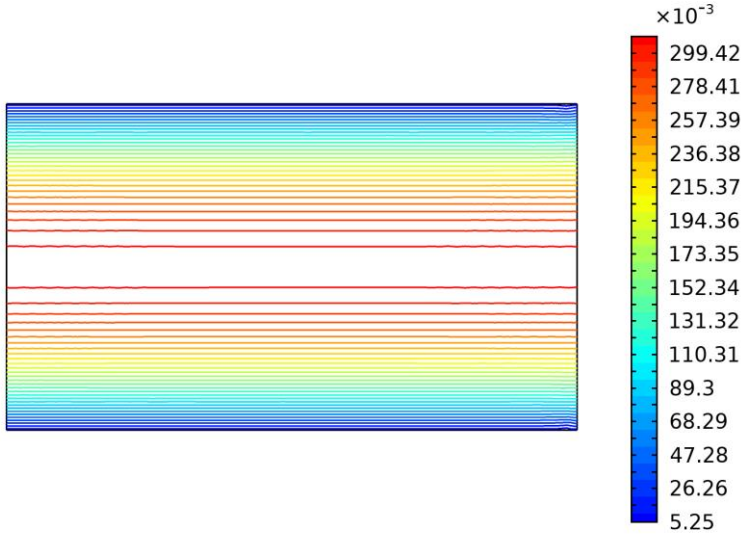

Figure A-12. *Velocity profile of fluid flow over the flat membranes*

About the Author

Dharmjeet Madhav, an Indian fellow who did his bachelor's studies in polymer science at Indian Institute of Technology (IIT) Roorkee (India), joined the Erasmus Mundus European master's programme in membrane engineering (EM3E-4SW) right after his graduation in 2018. He successfully completed the first three semesters while smoothly adapting to 3 different European countries where each semester was held.

University of Montpellier II (France) and University Paul Sabatier III (Toulouse, France) introduced him to the fundamentals of materials science and chemical engineering. Next, University of Chemistry and Technology Prague (Czech Republic), laid the foundations of membrane process modelling and technologies. Finally, University of Zaragoza (Spain), allowed for a specialization in nanoscience and nanotechnology. His curiosity guided him to conduct his master's thesis with the membrane technology group at KU Leuven (Belgium), led by prof. Ivo Vankelecom.

Preliminary to his thesis, Dharmjeet has always seized opportunities to do research: he synthesised and characterized cation and anion exchange membrane for his bachelor's thesis, later at university of Zaragoza, he synthesized the nanoparticles of zeolitic imidazolate framework ZIF-94 using inorganic deprotonators. He has been awarded with several scholarships and awards including merit cum means scholarship for his bachelor's studies at IIT Roorkee, Erasmus Mundus scholarship for his master's in membrane engineering and travel grant award from European membrane society to attend EMS summer school 2019 in the University of Edinburgh, UK.

Dharmjeet aspires to carry on his research career in the field of membranes and polymer technology, while always serving his surrounding and reaching out to new cultures.

Email: dmrnj1@gmail.com